A Comparative Study of Different Deep Learning Algorithms for Urinalysis Recognition System

A Thesis

Submitted to the Council of the College of Technical Engineering at Erbil Polytechnic University in Partial Fulfillment of the Requirements for the Degree of Master of Information Systems Engineering

By

Zhwan Mohammed Khalid

BSc. Software Engineering

Supervised By

Dr. Roojwan Sc. Hawezi

Dr. Sara Raouf Muhamad Amin

Erbil Kurdistan

October 2022

بسم الله الرحمن الرحيم

يَرْفع اللـه الـدِين آمَنُوا مِنكُمْ وَالَّذِين أُوتُوا الْعِلْمَ دَرَجَاتٍ وَاللَّهُ بِمَا تَعْمَلُونَ خَبِر

DECLARATION

I declare that the Master Thesis dissertation entitled: (**A Comparative Study of Different Deep Learning Algorithms for Urinalysis Recognition System**) is my own original work, and hereby I certify that unless stated, all work contained within this thesis is my own independent research and has not been submitted for the award of any other degree at any institution, except where due acknowledgment is made in the text.

Signature:

Student Name: Zhwan Mohammed Khalid

Date: /   / 2022

LINGUISTIC REVIEW

I, hereby, certify that this thesis, titled "**A Comparative Study of Different Deep Learning Algorithms for Urinalysis Recognition System**" has been read and checked. After indicating all the grammatical and spelling mistakes, the thesis was given again to the candidate to make adequate corrections. After the second reading, I found that the candidate corrected the indicated mistakes. Therefore, I certify that this thesis is free from mistakes.

Signature:

Name: Rozhgar Yusf Omer

Date: /   / 2022

SUPERVISOR CERTIFICATE

This thesis has been written under our supervision and has been submitted for the award of the degree of Master of Engineering with our approval as supervisors.

Signature: Signature:

Name: Dr. Roojwan Sc. Hawezi   Name: Dr. Sara Raouf Muhamad Amin

Date: /   / 2022   Date: /   / 2022

I confirm that all requirements have been fulfilled.

Signature:

Name: Dr. Roojwan Sc. Hawezi

Head of the Department of Information Systems Engineering

Date: /   / 2022

I confirm that all requirements have been fulfilled.

Postgraduate Office

Signature:

Name:

Date: /   / 2022

EXAMINING COMMITTEE CERTIFICATION

We certify that we have read this thesis: (**A Comparative Study of Different Deep Learning Algorithms for Urinalysis Recognition System**) and as an examining committee examined the student (Zhwan Mohammed Khalid) in its content and what related to it. We approve that it meets the standards of a thesis for the degree of Master of Engineering.

Signature:
Name: Prof. Dr. Raghad Z. Yousf
Member
Date**:**   /   / 2022

Signature:
Name: Assist. Prof. Dr. Shavan Askar
Member
Date**:**   /   / 2022

Signature:
Name: Prof. Dr. Yazn A. Xalil
Chairman
Date**:**   /   / 2022

Signature:
Name: Dr. Roojwan Sc. Hawezi
Supervisor 1
Date**:**   /   / 2022

Signature:
Name: Dr. Sara Raouf Muhamad Amin
Supervisor 2

Date**:**   /   / 2022

Signature:
Name: Assist. Prof. Dr. Ayad Zaki Sabr
Dean of the College of Erbil Technical Engineering
Date**:**   /   / 2022

DEDICATION

I dedicate this thesis to

- My family.
- Erbil Polytechnic University Staffs.
- All who supported me.

ACKNOWLEDGMENTS

ABSTRACT

Urine microscopic examination is critical for the diagnosis and monitoring of individuals suspected of having renal disorders or urinary tract infections. Traditionally, urine sediment smears are examined under a microscope for manual counting and categorization of urine sediments. This makes a time-consuming and labor-intensive process. Also it is susceptible to human mistakes and the skill of the human observer, and cannot satisfy today's clinic requirements. Clinicians and patients would benefit greatly from an automated method that can analyze and quantify urine sample images.

In this study a deep learning method is proposed for analyzing urinary particles. In the first step microscopic images of urine sediment ware collected in real human urine, which combined 820 images for four cell classes: Red Blood Cell (RBC), Calcium Oxalate, Cysten, and Uric acid. Then some preprocess on images to be specified and clearer are provided to get a good result. In the next step for classification and analyzing urine sediment two methods are presented. In the first method after making preprocess the image directly goes to classification algorithms, for this method Convolution Neural Network (CNN) structure and five ConvNet models such as MobileNet, VGG16, DenseNet, ResNet50V, and InceptionV3 have been proposed. Therefore, in the second method before images go to classification algorithms feature extraction is performed. 22 features from the images are extracted, and then numeric dataset is prepared and normalized it. Lastly, the normalized dataset have been introduced to the classifiers to distinguish subjects. For that purpose two different classifiers have been employed including Support Vector Machine (SVM) and K-Nearest Neighbor (KNN). After performing these two ways by using eight classification models and Training on the real dataset, it was realized that the best model is MobileNet. This model achieved the highest accuracy of 98.3%. Also, InceptionV3 and DenceNet have comparable accuracy results with 97.5%. And the proposed CNN structure has a good result with 96.12%. This study will be greatly beneficial for clinicians to automate, analyze, and quantify urine sediment images.

TABLE OF CONTENTS

Contents

LIST OF TABLES

LIST OF FIGURES

LIST OF ABBREVIATIONS

AC	Accuracy
ANN	Artificial Neural Network
AFA	Area Feature Algorithm
CNN	Convolution Neural Network
CAKUT	Congenital Abnormal Kidney and Urinary Tract
CaOx	Calcium Oxalate
DCNN	Deep Convolutional Neural Networks
DMCNN	Deep Multiscale Convolutional Neural Network
EC	Epithelial Cell
FN	False Negative
FP	False Positive
FPN	Few layers of networks
GPU	Graphics Processing Units
HOG	Histogram of Oriented Gradient
KNN	K- Nearest Neighbors
Min	Minimum
Max	Maximum
mAP	Mean Average Precision
MRI	Magnetic Resonance Imaging
OCT	Optical Coherence Tomography
PCD	Probability Correct Detection
RBC	Red Blood Cell
ReLU	Rectified Linear Unit
R-CNN	Regions with Convolutional Neural Networks
SVM	Support Vector Machines
SSD	Single Shot Multi-Box Detector
TN	True Negative
TP	True Positive
US	Urine Sediment
USE	Urine Sediment Examination
VGG	Visual Geometry Group
WBC	White Blood Cell
WSIs	Whole Slide Images

CHAPTER ONE
INTRODUCTION

1.1 OVERVIEW

Urinalysis is essential for the accurate identification of renal and urinary tract disorders. Its goal is to gather information on the number of particles in urine sediment, which is mostly consisting of calcium (Oxalate, cysteine, uric acid, Phosphate), mucus, Blood Cells such as red blood cells and white blood cells, and Casts(Lamchiagdhase et al., 2005, Lakatos et al., 2000). Urine sample analysis is critical in clinical screening, diagnosis, and public health promotion. Because a patient's urine sample differs from that of a healthy individual, the analysis can successfully aid in the identification of urinary problems. In general, the RBC count may be used to detect disorders associated with haematuria, Inflammation of the kidneys and bladder, renal tuberculosis, and other conditions(Lamchiagdhase et al., 2005, Lakatos et al., 2000).

Urinalysis has long been one of the most common tests used to diagnose sickness and diseases. The majority of laboratories follow the same urinalysis process, which involves the use of chemical test strips, urine sediment microscopy, and urine flow cytometers (Wu et al., 2010). Urinalysis is most commonly used to identify the presence of chemical compounds in urine, which may be accomplished with urine dipstick reagents. After dipping a stick in a urine sample, the response color of each reagent is visually compared to the dipstick color chart (Ginardi et al., 2014). Besides, it can be used to show a variety of physiological functions. Urinalysis is a crucial procedure used to identify a variety of conditions, including kidney illness, kidney infection, prostate inflammation, diabetes, infectious disease, syphilis and glycosuria (de Boer et al., 2017). Urine tests are frequently used to assess if the body has a disease by qualitatively identifying urine sediment cells as well as quantitatively evaluating cell kinds, quan-

tity, and shape using microscopy. Higher erythrocyte pee looks pale in the urine test; however, the presence of hematuria may be noticed under a microscope. If the leukocyte count is high, the majority of the examiners have urinary system infections; if abnormally shaped erythrocytes appear in the urine microscopy, the patients have most likely pain from kidney disease; and if the urine microscopy confirmed epithelium cells, the patients renal parenchyma has been destroyed and requires treatment.(Dong et al., 2020).

Urine microscopic images are distinguished by a range of particle types, and because the particles are small and irregularly dispersed, urine microscopic analysis necessitates the use of skilled laboratory physicians. Furthermore, urine analysis is time-consuming and labor-intensive, and it is easily impacted by laboratory physicians' subjective will and fatigue. With the evolution of digital image technology, automatic image categorization has grown in popularity in the medical field. The traditional approach, based on "target segmentation feature selection and extraction classifier," has made some success in identifying and detecting urine sediment pictures(Almadhoun and El-Halees, 2014). The usefulness of these strategies is mostly determined by the accuracy of target segmentation and the efficiency of feature selection and aggregation. Urine sediment photographs include less distinguishing elements apparent to the human eye when compared to other common images, and certain categories have a high degree of similarity. As a result, breaking past the bottleneck of high-accuracy classification using standard approaches is difficult. Deep learning technology has advanced significantly in recent years, especially to the fast growth of high speed computer hardware such as Graphics Processing Units (GPU) (Wäldchen and Mäder, 2018)

1.2 MICROSCOPIC URINALYSIS

The examination of a urine sample is referred to as urine analysis. This test is often used to diagnose a variety of disorders and follow-up of people who are suspected of having renal diseases or urinary tract infections. (Oyaert and Delanghe, 2019).

For microscopic urine testing, the first morning test is the recommended test. Because of the amount of time it existed, it is usually more concentrated. As a result, if such analyses as proteins or other biological constituents are present, the sample will include substantially greater concentrations of them (İnce et al., 2016).

The urine sample is simply poured into a test tube and centrifuged to perform microscopic urinalysis (spinning it down in a machine). The gathered substances are then examined and counted under a microscope (Velasco et al., 2019). Figure 1.1 shows the process of preparing urine sediment in a 10 mL test tube, the urine is centrifuged at 2,000rpm for a few minutes. The supernatant (9 mL) is discarded. A slide is pipetted with 1mL of sediment. The coverslip is applied and examined, staining or not. If the macroscopic analysis is negative, the microscopic examination is postponed. The degree of analysis, however, is determined by the clinical state. (Wesarachkitti et al., 2016). The content of Urinary Sediment (US) is shown in Table1.1 for this study four types of urine sediment are focused on which are RBC and three types of Crystals. Having blood in your urine is typically not a cause for concern. However, red blood cells and crystals in your urine may indicate the presence of a medical problem that requires treatment, such as a urinary tract infection (UTI), kidney illness, or liver disease (Cao et al., 2009).

CENTRIFUGATION

↓

RESUSPENSION OF SEDIMENT

↓

SLIDE PREPARATION

↓

MICROSCOPIC EXAMINATION
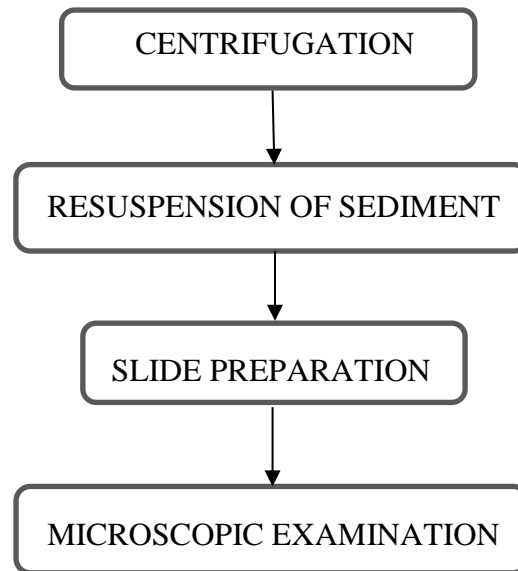
Figure 1. 1 Preparation for Analyzing Urine Sediment(Wesarachkitti et al., 2016)

Table 1. 1 Different subject were detected in the US study.

Class	Associated Conditions
Red Blood Cell	May be a normal finding in patients who play contact sports
Crystals	Large number of crystals in urine puts you under the risk of getting kidney stones later. 1. Calcium oxalate crystals. 2. Cysteine crystals. 3. Uric acid crystals.

1.3 IMAGE ANALYSIS

The urine sediment image is influenced by a number of elements while being processed in a unique urine sediment microscopic environment, there are multiple artifacts and noise in the images, reducing image quality and complicating the classification stage. The following characteristics distinguish urinary sediment images from natural images (Shen et al., 2017):

1. Contrast is low: Because the borders of some urine sediments are blurred, contour recognition is prone to fracture, as demonstrated in Figure 1.2 (a).

2. Weak edge: Because the urine sediment is not really positioned on the microscope's focal point, the "weak edge" occurrence manifests itself in the urine sediment border, as seen in Figure 1.2 (b).

3. Background effect: Because of depth of field emission, components outside the Field of View (FOV) generate hazy "diffusions," as seen in Figure 1.2 (c).

4. Adhesion: As indicated in Figure 1.2 (d), there are many cell breakages and overlapping adhesions, which complicate future separation and have a significant influence on the quantitative measurement of cell counts and associated factors.

To avoid above artifacts and noise in the medical images, some preprocessing on the images is needed before going to scanning algorithms to be classify them, such as in this study Grayscale and threshold operation are performed.

a) Contrast is low   **b) Weak edge**

c) Defocusing   **d)** Adhesion
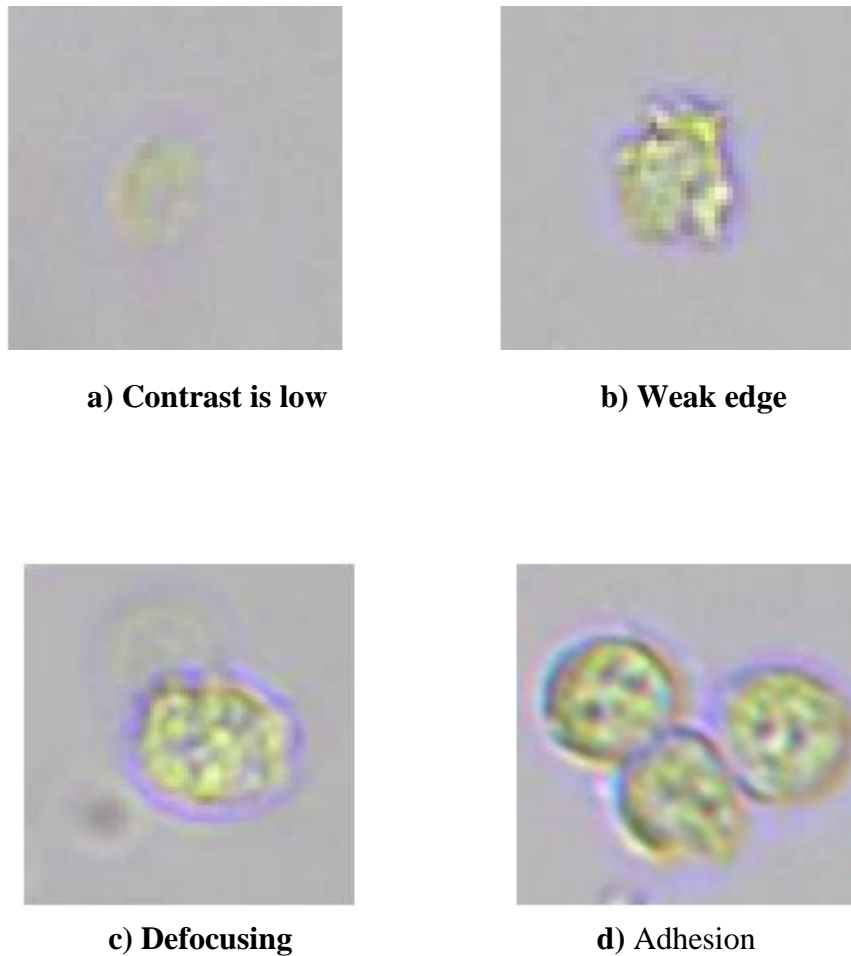
Figure 1. 2 Urinary sediment image features.

1.4 PROBLEM STATEMENT

urine sediment images have fewer distinctive features visible to the human eye and high similarity among some categories. Thus it is difficult to break through the bottleneck of high-accuracy classification using traditional methods. urine microscopic examination requires experienced laboratory physicians to operate. Moreover, urine analysis has a large workload and is very time-consuming, and can be easily affected by the subjective will and working fatigue of laboratory physicians and error prone. With the continuous development of digital image technology, automatic image recognition has been widely used in the field of medicine

1.5 THESIS AIMS

This thesis aims to design and evaluate the algorithms that implemented to recognition urinary sediment images and to choice the algorithm that, preferably, enhances the test outcomes of state-of-the-art urine sediment classification algorithm. As well as, to investigate the usage of deep learning techniques in the medical field, specifically in urinary sediment image classification. The implementation of deep learning in the medical domain can help:

• Either in giving a second opinion or giving assistance to the laboratories in classifying urinary sediment images.

 • To facilitate the process of image classification and to make it more accurate.

1.6 OBJECTIVES

1. Determine the best method for doing accurate computer-aided microscopic urine analysis.
2. Take a number of original urine sediment images with high resolution for various particles that is fit to handle deep learning.
3. Identify the best strategy for preprocessing images of microscopic urine samples.
4. Extract the best features of the observed objects that yield greatest classification rates.
5. Research the optimal classification model for categorizing urine particles.

1.7 THESIS OUTLINES

There are five chapters in this thesis. Below is an outline of the following chapters' concepts:

Chapter 1 contains a general introduction and a brief description of the subject, highlighting the problem statement, aims, objectives, and outlines.

Chapter 2 provides the background theory and information required to understand many new tools and technologies used in them. It provides a literature review from different articles, journals from various conferences, and websites.

Chapter 3 outlines the architecture of the proposed approach and the related algorithms.

Chapter 4 outlines all results of proposed methods, with the required evaluation methods.

Chapter 5 includes the conclusion, scope and limitations of this study and future recommendations.

CHAPTER TWO

LITERATURE REVIEW AND BACKGROUND THEORY

2.1 INTRODUCTION

Urinary particles are critical components of clinical urinalysis, particularly in the diagnosis and treatment of patients suspected of having renal illnesses or urinary infections. Because of that reason various techniques have been proposed to detect and classified urine sediment images, some of the approaches have succeeded and have a good result. This chapter reviews some of the previous studies that are done on urine sediment images. Also in this chapter the theoretical basis and the basic rules that have been needed for achieving urine sediment classification are discussed.

2.2 LITERATURE REVIEW

Based on CNN many researchers proposed an approach regarding urine sediment analyses, in 2018 Kang et al. proposed two state of art (Faster R-CNN and Single Shot Multi-Box Detector (SSD)). This method evaluated on a dataset consist of 5, 378 image samples corresponds of 7 type of urine sediments, such as RBC, WBC, Epithelia cell, epithelia nuclei, crystal, cast, mycete. They achieve best result of mAP 84% (Kang et al., 2018).

In 2018, Pan et al. classified and categorized RBC, WBC and Calcium Oxalate Crystals. They used large dataset and break the original convolution neural network's limitations. Cropping the input image first, and all images are created the same size because of the Convolution neural network's input layer is of the same size of input Image. Then they used dropout method to generate sub-graph to improve sample diversity without avoiding fitting generation. They obtained classifi-

9

cation lose rate in test set and train set, the accurate rate of their classification is 97 percent (Pan et al., 2018).

Liang et al. presented the DFPN approach in 2018 to handle class misunderstanding in Urine Sediment Examination (USE) images, which is difficult to correct using the baseline model They investigated the significance of two baseline model components in locating USE cells. To begin, adding an attention module and a class-specific attention module to the network head improved mAP by 0.7 points with a pre-trained ImageNet model and 1.4 points with a pre-trained COCO model. DenseNet was then merged into the USE baseline model (DFPN) for cell detection, resulting in the network's head input including several levels of semantic information, whereas the baseline model only provides high-level semantic information. After balancing the categorization and leaping regression losses, DFPN obtains the best performance with a mAP of 86.9 percent on the USE test set (Liang et al., 2018b).

In 2018, Liang et al. Faster RCNN and a convolutional neural network (CNN) were utilized to learn features from start to finish in order to recognize urine particles. They regarded urine particle detection as object detection and used two cutting-edge CNN-based object detection methods, Faster R-CNN and single shot detector (SSD), as well as urinary particle recognition variants. The authors next investigated numerous aspects influencing these CNN-based techniques in order to increase the accuracy of urine particle detection. They rigorously evaluated their methods on a dataset of 5,376 annotated images reflecting seven urine particle categories. They achieve the highest mean average accuracy (mAP) of 84.1 percent while taking just 72 seconds each image (Liang et al., 2018a).

The findings of the UriSed 3 and UX-2000 automated urine sediment analyzers, as well as the human microscopic technique, were compared in 2018. Two automated urine sediment analyzers, UriSed 3 and UX-2000, were used to assess 277 samples of residual fresh pee. Both devices' results indicated great agreement for quantitative assessment of red and white blood cells. The UX-2000 had a lower coefficients correlation and slightly inferior agreement with squamous epithelial cells. Semiquantitative analysis revealed that both machines had excellent concordance, with all significant rates falling within one grade difference of the other. Although UX-2000 was more sensitive to bacteria and hyaline casts, UriSed 3 was more sensitive to tiny spherical cells (Laiwejpithaya et al., 2018).

In 2018, Sun et al. suggested a method for identifying RBCs in urine sediment micrographs that makes use of aggregate channel features and soft-cascade adaboost Quick feature extraction and a big representation capacity are two advantages of aggregate channel characteristics. They provide a method that does not require any picture segmentation beforehand. Researchers amass a collection of micrographs of urine sediment. They discovered that their proposed strategy is more accurate and faster, for identifying RBCs in urine sediment micrographs. The technique based on Histogram of Oriented Gradient (HOG) combines with Support Vector Machine (SVM) (Sun et al., 2018).

In 2018, Jiang et al. suggested a method for segmenting urine sediment images in 2018 using 20-fold magnification microscopy and the Markov model. This approach uses the sum average feature produced from the spatial gray co-occurrence matrix for classification in the 77-neighborhood window. To begin, each pixel in the image is evaluated based on its intensity dispersion in comparison to the average intensity of its 77 neighbors, with pixels with larger dispersion being processed further using the Gaussian mixture model. To generate comparable results, the weights are integrated into a feature distance matrix inside the window, allowing the features to be re-estimated. The required PCD (Probability of Correct Detection) is 94%..(Jiang et al., 2018).

In 2018, Rahmat et al. a color categorization system for urine dipstick images is offered. The color image of the urine dipstick was obtained using a scanner by the authors. Because the light generated by a scanner is continuous, it may be utilized to analyze urine dipstick data. To overcome the problems of manual urine dipstick color matching and test reference color, a technique is necessary. The authors recommend using Euclidean Distance, Otsu, and RGB color feature extraction to match the colors on the urine dipstick with the standard urine examination color. The findings demonstrate that the proposed method categorized the colors on a urine dipstick with a 95.45% accuracy (Rahmat et al., 2018).

In 2019, Xiang et al based on the entire convolution neural network, and proposed a new identification approach for microscopic examination of CaOx crystals in urine samples. This method can detect the image of a microscopic examination of CaOx crystal calculation automatically, and the artificial recognition rate with clinical professionals is as high as 74% (Xiang et al., 2019).

In 2019, Cruz et al. The algorithm of Canny Edge Detection with the Circular Hough Transform was utilized in image processing to count WBCs and RBCs in a urine sample. There are two (2) stages to the procedure. Canny Edge Detection is the first component, while Circular Hough Transform techniques are the final. It reveals that the proposed technique has at least a 93.2% accuracy when compared to the actual RBC and WBC count findings (Cruz et al., 2019)

In 2019 Ji et al. employed enormous urine sediment pictures for training, the network model which uses 300,000 samples for recognizing 10 categories. They solved the difficulty of CNN by applying the area feature algorithm (AFA), which may lessen the area feature of the input picture. They achieved 97% accuracy in the test set. (Ji et al., 2019).

In 2019, Zhang et al. the residual network is utilized to build the convolutional network, which extracts urine sediment features from several views. To minimize network parameters, depth wise segmented convolution is utilized. Follow-

ing that, a Squeeze-and-Excite block is used to learn feature weights, which is followed by feature re-calibration to improve network representation and spatial pyramid pooling to increase network robustness. Finally, the Adam with weight decay optimization approach is employed to speed network model convergence in order to improve recognition results even more (Zhang et al., 2019).

In 2019, Li et al. give a straightforward method for detecting and recognizing casts in urine sediment images. They employed urine casts as the detection object in urine microscopy and then transferred it to the ResNet50 network; feature maps of varied sizes can be acquired in the network's final layers (FPN). Finally, they feed individual target area feature maps into classifier subnetworks for classification and segmentation, and the detection results are returned. According to statistics, the average precision of the recognition result is 89.4% (Li et al., 2019b).

In 2019, Zheng et al. deep transfer learning algorithms were tested for their diagnostic accuracy in distinguishing normal children's kidneys from those with congenital kidney and urinary tract abnormalities (CAKUT). The researchers used a transfer learning algorithm to evaluate kidney properties from ultrasound pictures gathered during normal clinical treatment of 50 children with CAKUT and 50 controls. Support vector machine classifiers were trained to identify between sick and normal kidneys based on the acquired features. According to the findings, classifiers based on transfer learning features and traditional picture characteristics could discriminate abnormal kidney pictures from controls with an accuracy of higher than 0.88 (Zheng et al., 2019).

In 2019, Wang et al. in urine sediment images, they investigated crystal segmentation and recognition techniques. Crystalline particles, RBC, WBC, epithelial cells, and tubular cell samples were used in the study; this study proposes an integrated technique for detecting and characterizing crystalline components in urine microscopic particles. To begin, the canny operator is used to identify and locate particles, followed by MRF segmentation to recover the target object's strong textural structure, which aids in the extraction of following identification

characteristics. The Sector statistical Fourier descriptor is a unique shape feature that, along with the corner and circularity features, is utilized to construct the feature vector for the SVM classifier (Wang et al., 2019).

In 2019, Teng, Li, and Karim present a novel deep multiscale convolutional neural network (DMCNN)-based model for brain (MRI) picture segmentation. Raw medical photos were used to extract the region of interest. Data augmentation is then used to obtain additional training datasets. Three models are proposed in the technique: encoder, U-net, and decoder. The encoder is primarily in charge of extracting features from 2D picture slices. The U-net combines the properties of each encoder block with those generated via deconvolution in various-sized decoders. After feature extraction, decoding is largely responsible for up sampling the feature graph for each group. The model results show that the new method improves segmentation accuracy. Furthermore, as compared to other materials, it has a high level of resilience (Teng et al., 2019).

In 2019 Sanghvi et al. create a method for reporting urine cytopathology using artificial intelligence. They scanned 2405 vintage ThinPrep glass slides with urine cytology cases that have been voided and instrumented. To evaluate whole slide images (WSIs) and forecast diagnoses, a deep learning computational pipeline with various tiers of convolutional neural network models was constructed. To verify the approach, a unique test data set of consecutive patients seen in routine clinical practice was employed. A total of 1.9 million urothelial cells were examined. Each WSI had 5400 urothelial cells on average. The approach yielded a 0.88 area under the curve. The algorithm's sensitivity for high-grade urothelial cancer was 79.5 percent. When utilizing the optimal operating point, specificity was 84.5 percent.(Sanghvi et al., 2019).

In 2019, Wahid et al. CNN-SVM, CNN-KNN, and CNN-Nave Bayes are three hybrid models based on transfer learning approaches that were introduced. In this strategy, CNN was used as an automated feature extractor. In CNN-SVM, CNN-KNN, and CNN-Nave Bayes hybrid models, SVM, k-NN, and Nave Bayes

classifiers are employed for classification, respectively. Many internet microbiology image sources, including PIXNIO and HOWMED, were used to collect microscopic photos of the selected bacterium species (Sajedi et al., 2020). The usefulness of these suggested hybrid models was investigated, and the hybrid CNN-SVM model with the highest accuracy (98.7 percent) was identified, showing that the hybrid model is a viable classification strategy for microscopic bacteria photo classification (Wahid et al., 2019).

In 2020, Li et al. used the ResNet50 network to distinguish seven types of detection objects in microscopic imaging of urine sediment. They retrieved features with Resnet50, and feature maps of various sizes were created in the feature pyramid net's final layers (FPN). To get detection results, the feature maps are subsequently transmitted to the classification and regression sub networks for categorization and localisation, respectively. The optimum network architecture was created by adjusting the loss functional parameters, which resulted in the best outcomes in the urine particle test set. The accuracy of the experimental results was 88.65% (Li et al., 2020b).

In 2020, Liu, Li, and Gong to categorize the tiny images of urine sediment, a fine-tuned CNN ensemble was utilized. As a preprocessor, the FCN has been utilized to segment raw urine sediment microscopic pictures into urine sediment microscopic images with just one target per image. The ResNet50, GoogLeNet, and AlexNet were ntegrated as an ensemble of CNNs to extract more discriminant features, and an FNN was utilized as a classifier to offer classification results. Experiment findings revealed that their proposed technique outperformed existing state-of-the-art technology (Liu et al., 2020).

In 2020 Li et al. images of urine erythrocytes were taken using an optical microscope. A total of 3969 urine images were collected using a data augmentation approach. Erythrocytes, which occupied the space, left by domestic urine, Erythrocyte datasets. The results of the trials show the method described here can detect five different types of urine erythrocytes which were 99.8 percent. (Li et al., 2020a).

In 2020, Dong et al. evaluated the urine sediment apparent component and was detected utilizing a deep learning-based edge object detection technique. On the urine sediment visible component dataset, they enhanced the detection accuracy of the YOLOv3 method. The dataset trial results show that the revised YOLOv3 has increased detection accuracy with five different types of urine sediment components. The results demonstrate that their technique achieves the highest mean average precision (mAP) of 90.1 percent, with an average detection time of 0.047s per frame (Dong et al., 2020).

In 2020, Goswami et al. deep learning algorithms were described for automating the identification and categorization of red blood cells, pus cells, and other cells. It also detects clusters of these cells, which might suggest major issues such as urine infection (as evidenced by the presence of pus cells and clusters), kidney stones, and other disorders. They created an annotated database of tiny pictures of urine sediment particles, which might potentially accelerate biomedical imaging studies. On this dataset, the YOLOv3 and RetinaNet models were trained, and they may be utilized to distinguish and classify cells in urine samples for medical diagnosis (Goswami et al.).

In 2020 Wang et al. demonstrated a two-stage urine sediment detection technique. Specifically, segmentation and classification problems are transformed into object detection challenges, with Deep Convolutional Neural Nets extracting features (DCNN). HOG+SVM were employed as a region recommendation in our technique, and Trimmed MobileNets were used to refine DCNN. The research used a total of 56900 samples. The experimental findings indicate that the proposed method yields good outcomes (Wang et al., 2020).

In 2020, Balbin et al. created a Raspberry Pi program to distinguish and classify triple phosphate crystals and calcium oxalate crystals, as well as other objects detected on a microscopic image of urine sediment. The Harr feature was used to define the edges of the crystals, while AdaBoost and SVM were used to classify and categorize the crystals discovered in urine sediment using OpenCV.

The actual testing results show that the objectives were met, and the system was capable of recognizing and classifying both crystals analyzed. Both crystals achieved higher than 90% accuracy (Balbin et al., 2020).

In the year 2020, Li et al. developed a deep learning approach for identifying and categorizing recognized aspects in urine sample images based on the LeNet-5 network. Shape analysis is used to identify and categorize items in urine samples viewed under microscopes. The LeNet-5 neural network was modified by increasing the number of output nodes while decreasing the number of convolutional layers. They also compared their approach's outcomes to those of regular feature extraction followed by back-propagation neural networks. Their research revealed that their approach was more exact, sensitive, and specific. The method's performance shows that it has several applications in urine sample analysis.The suggested approach can identify RBCs and WBCs with a 90 percent accuracy rate (Li et al., 2020c).

In 2021, Qu et al. presented an automated urine sediment image recognition approach to begin, annotate, and pre - process urine sediment images in order to create a urine sediment data collection. In order to respond to the deep learning model's input, the super-resolution reconstruction technique is employed to duplicate the small-size urine sediment picture. Finally, an hourglass residual network is built to automatically extract features from urine sediment images in order to conduct urine sediment image classification and identification. The method's total accuracy for recognizing 13 different types of urine sediment images can reach 99.05%, according to the findings of the testing (Qu et al., 2021).

In 2022, Wu and Ji a positive outcome may be obtained by employing 70,000 urine sediment images from the training set and 9,870 from the test set. The results of the tests show that the USNet model has an average classification accuracy of more than 93 percent for 14 different types of urine sediment images. They created a urine sediment picture recognition algorithm based on the VGG using the attention mechanism and structural re-parameterization. During training, a multibranch structure is built to improve identification accuracy while retaining the

benefits of VGG inference speed, and feature extraction is further aided by the attention mechanism, which successfully improves the classification impact of often confused categories (Wu and Ji, 2022).

Table 2. 1 comparison between previous studies and illustration of their result

Author	Method	Discussion	Result
(Kang et al., 2018)	CNN	Based on CNN, two cutting-edge techniques (Faster R-CNN and Single Shot Multi-Box Detector (SSD)) were presented.	Accuracy= 84%
(Pan et al., 2018)	CNN	By breaking the original convolution neural network's limitations can proved better result	Accuracy= 97%
(Liang et al., 2018b)	DFPN	DenseNet serves as the backbone network, increasing the mAP by 5.6 points over a strong baseline of FPN on Res-Net.	mAP = 86.9 %
(Liang et al., 2018a)	R-CNN acceleration and a single shot multibox detector (SSD)	The experiment detects seven types of urine sediment: erythrocytes, leukocytes, epithelial cells, crystals, casts, mycelium, and epithelial nuclei.	Accuracy= 84.1%
(Laiwejpithaya et al., 2018)	UriSed 3 and UX- 2000	Comparing between automated urine sediment analyzers and manual microscopic method	--------
(Sanghvi et al., 2019)	Deep learning computational pipeline with several convolutional neural network levels.	This service is used for automated Papanicolaou test screening and provides computer-assisted interpretation of urine cytology cases.	Specificity= 84.5%
(Sun et al., 2018)	HOG combined with SVM	suggested a method for identifying RBCs in urine sediment micrographs that makes use of aggregate channel features and soft-cascade adaboost	Accuracy= 96.68%

(Jiang et al., 2018)	Markov model	The Gaussian Mixture Model was used to evaluate features, while the Markov model was utilized to segment texture images.	PCD = 94%
(Rahmat et al., 2018)	Euclidean Distance, Otsu	Proposed an automated color categorization of urine dipstick images.	Accuracy= 95.45%.
(Xiang et al., 2019)	CNN	This method can detect the image of a microscopic examination of CaOx crystal calculation automatically, and the artificial recognition rate with clinical professional	Accuracy= 74%
(Cruz et al., 2019)	RCNN+ Vgg-Net	The algorithm of Canny Edge Detection with the Circular Hough Transform was utilized in image processing to count WBCs and RBCs in a urine sample.	Accuracy= 93.2%
(Ji et al., 2019)	CNN	By using area feature algorithm (AFA) they solved problem of CNN, which can weaken the area feature of input image	Accuracy= 97%
(Zhang et al., 2019)	Multi-view residual network	Method for Recognizing Urine Sediments in Microscopic Images Using Multi-View Deep Residual Learning	Accuracy= 90%
(Li et al., 2019b)	ResNet50	They utilized urine casts as the detection target in urine microscopy and then transferred it to the ResNet50 network; in the last few layers of networks (FPN),	Accuracy= 89.4%
(Zheng et al., 2019)	Transfer learning algorithm and SVM	Using ultrasound imaging data and combining textural image characteristics with deep transfer learning image features, computer-aided identification of congenital kidney and urinary tract abnormalities in children was performed.	Accuracy=0.88%
(Wang et al., 2019)	SVM	The Sector statistical Fourier descriptor is introduced as a new shape feature that works in conjunction with the corner and circularity features to build the feature vector for the SVM.	Accuracy=97.8%
(Teng et al., 2019)	deep multiscale convolutional neural network (DMCNN)	Three models are included in the proposed method: encoder, U-net, and decoder.	Hippocampus= 91.23 %

(Sanghvi et al., 2019)	Deep learning computational pipeline with several convolutional neural network levels.	This service provides computer-assisted interpretation of urine cytology cases, similar to the machine learning technology used for automated Papanicolaou test screening	Specificity= 84.5%
(Wahid et al., 2019)	CNN + SVM CNN + KNN CNN + Naïve Bayes	A Machine Learning Approach for Assessing the Performance of Microscopic Bacteria Image Classification.	Accuracy = 98.7%
(Li et al., 2020b)	ResNet50	Seven biological components were used as detection targets in urine microscopic imaging (i.e., RBC, WBC, epithelial, low-transitional epi-thelium, casts, crystal, and squamous cells cells)	Accuracy= 88.65%.
(Liu et al., 2020)	ResNet5, Goog-LeNet,and AlexNet were integrated as an ensemble of CNNs	As a preprocessor, the FCN has been utilized to segment raw urine sediment microscopic pictures into urine sediment microscopic images with just one target per image.	Accuracy= 96%
(Li et al., 2020a)	Faster RCNN in combination with VggNet	The results of the trials show the method described here can detect five different types of urine erythrocytes	Accuracy= 99.8%
(Dong et al., 2020)	YOLOv3	The dataset trial results show that the revised YOLOv3 has increased detection accuracy with five different types of urine sediment components	Accuracy= 90.1%
(Goswami et al.)	YOLOv3 and RetinaNet	Deep learning algorithms were described for automating the identification and categorization of red blood cells, pus cells, and other cells.	Accuracy= 78%
(Wang et al., 2020)	DCNN and (HOG+SVM)	Based on SVM and Trimmed MobileNets, a multiple urine sediment detection approach was presented.	Accuracy= 98.05%
(Balbin et al., 2020)	Harr Feature, Adaptive Boosting and Support Vector Machine	The Harr feature was used to define the edges of the crystals, while AdaBoost and SVM were used to classify and categorize the crystals found in urine sediment.	Accuracy = 90%
(Li et al., 2020c)	LeNet-5	Shape analysis is used to identify and categorize items in urine samples viewed under microscopes.	Accuracy= 90%

(Qu et al., 2021)	residual hour-glass structure and super-resolution image reconstruction	In order to adapt to the deep learning model's input, the super-resolution reconstruction approach was used to restore the small-size urine sediment image.	Accuracy= 99.05%
(Wu and Ji, 2022)	VGG	They used the attention mechanism and structural re-parameterization to create a urine sediment image identification algorithm based on the VGG.	Accuracy= 93%

2.2.1 DISCUSSION

Medical imaging, with the improvement of medical imaging technologies and the ongoing development of artificial intelligence image processing, may make or break a medical assessment. Medical image processing technology has evolved into an important component of research. Deep learning networks are transforming patient care and are playing an important role in clinical practice for health systems. The most often utilized deep learning techniques in healthcare include computer vision, natural language processing, and reinforcement learning. However, weak gray contrast and fuzzy tissue borders are frequently seen in medical images. Medical image segmentation accuracy cannot be significantly increased. Deep learning methods, in particular, need a greater number of training examples, resulting in a time-consuming approach. The above section and Table 2.1 contains a tabular display of more urine analysis-related research. This literature reviewed the several methods used for automatic recognition of urine particles, including RBC, WBC, crystals, casts, epithelial cells, bacteria, etc. from microscopic images of urine sediments. The traditional manual recognition method makes errors in the recognition and it is a time consuming process. A conventional method for urinalysis requires data pre-processing followed by feature extraction and classification. It requires fewer amounts of data compared to deep learning methods and considerable results have been obtained by using this method.

However the pre-processing and feature extraction stage in the machine learning based classifier will give some biased results. Machine learning method heavily depends on the segmentation accuracy and the effectiveness of the hand-crafted features. The intricate characteristics of microscopic images make segmentation difficult or sometimes impossible. The hand crafted features also gives some false detection results. To avoid the handcrafted features and identifying the significant biomarkers from the urinary microscopic images the researchers utilized the deep leaning algorithms namely CNN, LSTM etc. The deep learning method does not require any handcrafted features and the hidden biomarkers are identified by the network to predict the exact urinary sediment particles. Urinalysis using various types of convolutional neural networks such as RCNN, Faster RCNN, MS-FRCNN, DensNet etc. gives good results. Even though the CNN doesn't requires pre-processing and handcrafted features, it requires large scale annotated dataset for training the networks and also these methods are computationally complex. Annotation of particles in a microscopic urine image requires well experienced pathologist and annotation on large scale dataset is a difficult and time consuming process. To avoid these limitations of annotation can use good focus of the CCD camera, because the accuracy of recognition is also affected by the focus of the CCD camera. When the focus is not clear, the imaging effect is poor, which has a certain influence on the recognition result

2.3 INTRODUCTION OF MACHINE LEARNING AND DEEP LEARNING

Machine learning is a fast growing field of computing algorithms that try to mimic human intelligence by learning from their surroundings. In the present era of so-called big data, they are regarded as the workhorse. Machine learning techniques have been successfully employed in a variety of fields. including pattern recognition (Bishop and Nasrabadi, 2006), computer vision (Apolloni et al., 2005), aerospace engineering (Ao et al., 2010), finance (El Naqa and Murphy,

2022), entertainment (Gong and Xu, 2007, Yu and Tao, 2013), and computational biology (Mitra et al., 2008, Yang, 2010), as well as biological and medical applications (Cleophas et al., 2013, Malley et al., 2011). More than half of cancer patients are treated with radiation therapy (lionizing radiation), and it is the major therapeutic choice in early stages of local disease. Radiotherapy is a complicated set of actions that not only span the time between consultation and treatment, but also guarantee that patients get the prescribed radiation dose and respond appropriately. These processes vary in difficulty and may involve multiple phases of sophisticated human-machine interactions and decision-making processes, which would normally invite the use of machine learning algorithms in helping to improve and automating these methods, such as radiological physics quality control, contouring and diagnosis planning, image-guided radiotherapy, respiratory motion control, treatment success design, and results analysis. Machine learning algorithms' ability to learn from their current environment and apply to previously unknown tasks may enable breakthroughs in radiation security and efficacy, resulting in more effective results (Wuest et al., 2016).

Machine learning tries to replicate how humans (and other intelligent beings) learn to understand sensory (input) data in order to achieve an objective. This objective may be a pattern recognition exercise in which the learner must differentiate between apples and oranges. Even though each apple and orange is unique, we can generally tell them apart. Instead of hard-coding a computer with numerous realistic apple and orange representations, it might be built to learn to recognize them by being exposed to genuine apples and oranges on a regular basis. This is a great example of supervised learning, in which each training sample of data input (color, shape, odor, and so on) is associated with a preset categorization label (apple or orange). When the entities to be classified have multiple variable properties within their own classes while keeping major distinguishing traits, it aids humans in dealing with similarities and differences. Above all, a respectable person should be able to identify a previously unseen apple or orange (Saravanan and Sujatha, 2018).

The unsupervised algorithm is a sort of machine learning. This may be like attempting to hit a bull's-eye with a dart. In the mechanism that regulates the course of the dart, the device (or human) has several degrees of freedom. Rather than attempting to encode the kinematics beforehand. For each trial, the kinematic degrees of freedom are modified such that the dart comes closer and closer to the target. The training is unsupervised since it does not associate a certain kinematic input configuration with a specific output. From the training input data, the algorithm generates its own route. Ideally, the taught dart thrower will be able to adapt the learned kinematics, for example, to changes in target position. Semi-supervised learning is a sort of machine learning in which some data is labeled but not others. In this case, the labeled portion can be utilized to help understand the unmarked section. This type of setting is more favorable to most natural processes and more closely resembles how humans acquire their talents (Mahesh, 2020).
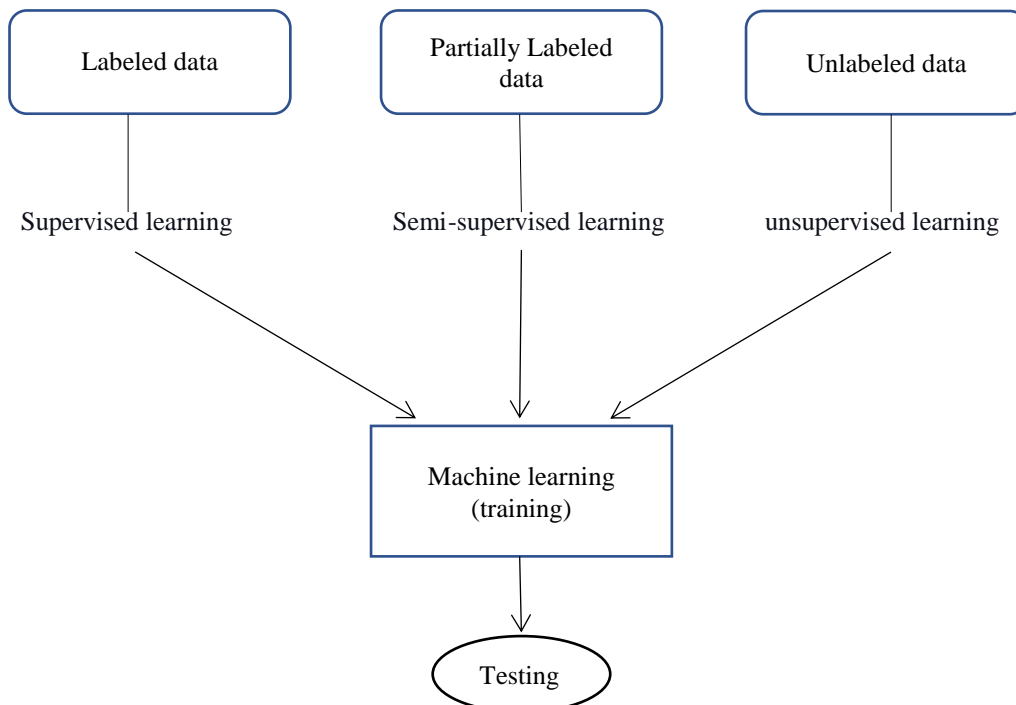

Figure 2. 1 Machine learning algorithms are classified based on the type of the training data (Mahesh, 2020).

The basic architecture for deep learning was inspired by the structure of a human brain in an effort to design systems that learn similarly to how humans learn. As a result, many essential terms in deep learning may be related to neurology. Deep learning design involves a processing unit known as a perceptron, which allows for the modeling of non - linear functions in the same way as neurons do in the brain. Deep learning's magic begins with the fundamental perceptron. The perceptron receives a list of input signals and turns them into output signals in the same way that a "neuron" in the human brain transmits electrical pulses throughout our nervous system (Madhavan and Jones, 2017).

The perceptron tries to understand data representation by layering different levels, each of which is in charge of processing a piece of the input. A layer is a group of computing units that learn to identify repeated occurrences of values. Each perceptron layer is in responsibility of comprehending a certain pattern in the data. The architecture is also known as neural networks because a network of these perceptions is similar to how neurons in the brain build networks (or arti-ficial neural networks) (Madhavan and Jones, 2017).

A brief explanation for each algorithm has written that have been applied on prepared dataset in below section discussed which are: CNN, SVM and KNN.

2.3.1 Convolution Neural Network

Deep learning has lately made substantial progress in a number of domains, and it is gaining popularity. CNN is one of the most widely used deep learning algorithms for analyzing visual data. Yann LeCun proposed the famous LeNet-5 in (LeCun et al., 1998), targeting at letter identification in postal offices and achieving good results. It is widely used in a variety of applications, for example, speech processing (Dahl et al., 2011), and computer vision(Krizhevsky et al., 2012). CNN has also made significant breakthroughs in medical fields. It has produced ground-breaking results in medical image recognition tasks such

as skin cancer (Esteva et al., 2017), optical coherence tomography (OCT) (Kermany et al., 2018), and chest X-rays (Meraj et al., 2019).

The network is made up of neurons that have weights and biases that vary dependent on the training data. It also has a local receptive field, which is a tiny patch of input layer neurons linked to hidden layer neurons. A convolutional layer, a pooling layer, and linked layers comprise the CNN structure (Ciregan et al., 2012). In CNN, feature extraction is performed by the convolutional and pooling layer, while mapping the extracted features into the final output is performed by the connected layer. The convolution layer is usually composed of combining nonlinear and linear operations, such as activation function and convolution operation. Convolution is used for feature extraction, which is a type of linear operation, and the outputs are then processed through a nonlinear activation function to improve feature extraction. The rectified linear unit is the most commonly used activation function (ReLU). The pooling layer applied to decrease the number of input parameters and reduce the dimensionality of the feature maps by performing down sampling operation. Once the feature extracted and down sampled, they mapped to the final outputs of the network by using a fully connected layer. Finally, activation functions such as sigmoid or softmax is applied to the last connected layer; this function is usually different from others because it requires to be chosen based on the tasks(Ciregan et al., 2012).

A convolutional network's initial layer is the convolutional layer. It is the last layer, even if extra convolutional layers or pooling layers might be added after the fully-connected layer. With each layer, the CNN becomes more complex, identifying more parts of the image. The first layers concentrate on essential aspects such as colors and borders. As they evaluate the visual data, the CNN layers learn to distinguish bigger components or attributes of the item, eventually recognizing the target object(Al-Saffar et al., 2017). They have three types of layers: convolutional, pooling and fully-connected (FC).

- **Convolutional Layer**

The convolutional layer serves as the foundation of a CNN and is where the majority of the processing takes place. A few components are required, including input data, a filter, and a feature map; the input is a color image with a three dimensional pixel matrix. This means that the input will have three dimensions: height, width and depth, which match to the RGB color space of an image. A feature detector, also known as a kernel or a filter, searches the image's receptive fields for the presence of a feature. This is known as a convolution (Albawi et al., 2017).

In the feature descriptor, a two-dimensional (2-D) weighted array offers a component of the picture. The size of the receptive field is normally set by a 3x3 matrix, regardless of the size of the filter. The data point between the input pix-els and the filter is calculated after connecting the filter to a section of the picture. After that, the data point is transferred to an output array. After that, the filter takes a step back and repeats the procedure until the kernel has completely covered the image. The ultimate result of a series of dot products from the input and the filter is a feature map, activation map, or convolved feature (Albawi et al., 2017).
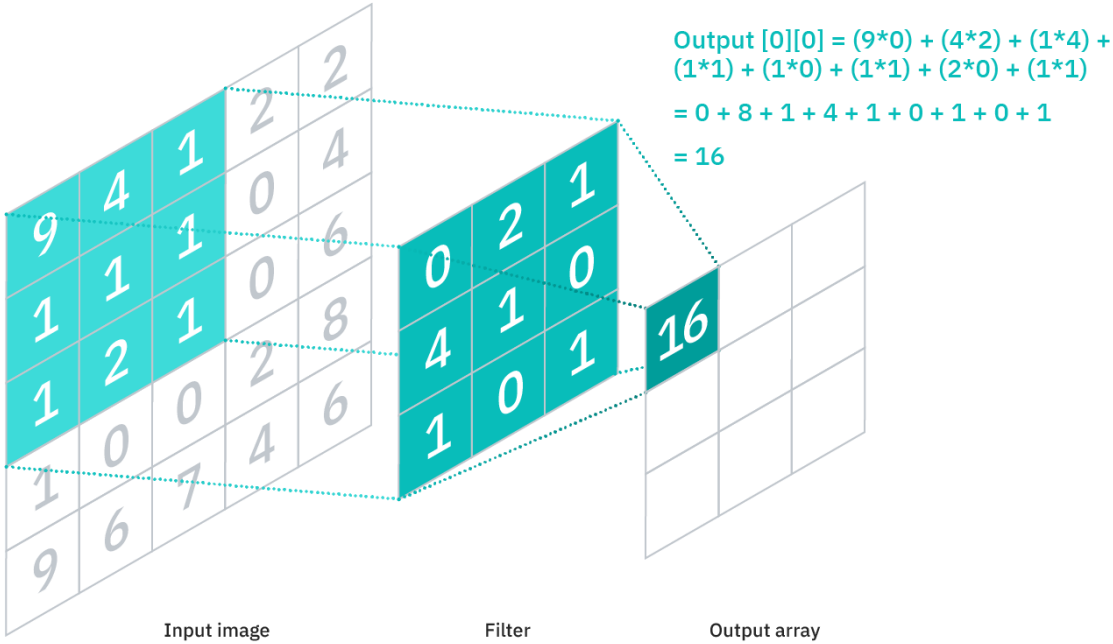
Output [0][0] = (9*0) + (4*2) + (1*4) +
(1*1) + (1*0) + (1*1) + (2*0) + (1*1)

= 0 + 8 + 1 + 4 + 1 + 0 + 1 + 0 + 1

= 16

Input image   Filter   Output array

Figure 2. 2 Convolution Layer Network (Albawi et al., 2017)

27

As illustrated in Figure 2.2, each feature output value does not have to correlate to each pixel value in the input image. It just has to be linked to the perceptron, where the filter will be applied. Convolutional and pooling layers are sometimes referred to as "partially connected" layers since the output array does not have to map entirely each input value. However, this attribute can also be given as a local link. It's worth noting that the feature descriptor's weights remain constant as it advances over the image, a technique known as parameter sharing. Back propagation and gradient descent cause some parameters, such as weight values, to change during training. However, before neural network training can begin, three important parameters that determine the output volume size must be established (Kim, 2017). These include:

1. The depth of the output is influenced by the filter size. Three distinct filters, for example, would produce three distinct feature maps with a depth of three.

2. The kernel stride is the number of pixels shifted across the input matrix. Although stride amounts of two or more are unusual, a larger stride leads in a lower capacity.

3. When the filters do not complement the input image, (0 padding) is often employed. In the absence of an input matrix, all components are set to zero, resulting in a larger or more evenly distributed output. There are three category of padding: No buffering, the same buffer, total padding (Kim, 2017).

- **Pooling layer**

Down sampling, also known as layer pooling, reduces dimensionality and hence the number of parameters in the input. Pooling, like the convoluted layer, sweeps a filter across the whole input without using weights. Instead, the kernel creates the output array by aggregating the receptive field input with an aggregation function. Pooling is classified into two types: maximum pooling and average pooling (Wang et al., 2017).

Although significant information is lost in the pooling layer, it does give certain benefits to CNN. They help with the reduction of complexity, the improvement of efficiency, and the decrease of the danger of overfitting.

- **Fully-Connected Layer**

The overflowing layer's name accurately depicts its function. In partly connected layers, as previously stated, the pixel values of the input picture are not directly related to the output layer. Each output layer node in the fully-connected layer, on the other hand, is directly related to a preceding layer node.

This layer categorizes the qualities obtained from the preceding levels as well as their numerous filters. While convolutional and pooling layers commonly utilize ReLu functions to categorize inputs, FC layers typically use a smooth activation function to generate a probability between Zero and one (Basha et al., 2020).

Convolutional Neural Networks may be put to use for computer vision applications in Deep Learning. When we deal with a huge dataset at that time, the model might take a long time to train. It might take many days or even weeks. In such instances, we can employ Transfer learning. In this study a pre-trained model is employed. There are currently numerous popular pre-trained models available for computer vision tasks.

- **Transfer Learning Model**

Pre-trained ConvNet models were employed in this analysis. They ware developed by F. Chollet. Transfer learning is a method of optimizing progress or performance while modeling the second task (Torrey and Shavlik, 2010).

Due to the massive processing power and time - frame necessary to process neural network simulations on these difficulties, it is a common deep learning method to use pre-trained models as the starting point for computer vision and natural language data processing (Torrey and Shavlik, 2010). By using Transfer learning technology, the network's weight can be initialized with a pre-training

model. The open-source Image net dataset is used to train the pre-training model, which contains 14.2 million images that have been successfully classified into 1000 categories. This is initiated and updated at random throughout training, with the exception of the whole connection layer; all network weights stay constant during the training period (Zhuang et al., 2020).

In this study five type of transfer learning model is performed on real dataset such as:

1. **MobileNet**

Tensor Flow's original mobile computer vision model, MobileNet, is designed for use in mobile applications, as the name implies. MobileNet employs depth-wise detachable convolutions. It considerably decreases the number of parameters when compared to the network with regular convolutions of the same depth in the nets. As a result, thin deep neural networks are being developed (Krishna and Kalluri, 2019).

.

2. **VGGNET**

VggNet was suggested by Karen Simonyan and Andrew Zisserman(Simonyan and Zisserman, 2014) . VggNet is a simple deep learning network that excels in image identification. VGG investigates the relationship between the depth and efficiency of convolutional neural networks. A 16–19-layer deep convolution neural network is built by stacking three small convolution kernels and two maximum pooling layers.

VGG16 is made up of Thirteen convolutional layers, three completely connected layers, and five pool layers. In the pool layer, a 2 2 filter is employed. More nonlinear mapping operations may be conducted by lowering the network parameters, improving the model's ability to fit. The VGG16 network came in second place in the 2014 ILSVRC (ImageNet Large Scale Visual Recognition Challenge)However, in a number of migrating learning tasks, it outperformed the champion (GoogLeNet) (Song et al., 2019). The original VGG16 network's convolutional neural networks were pre-trained with the

ImageNet dataset and fine-tuned with the urine erythrocytes training dataset.

3. InceptionV3

It's the third iteration of Google's Inception Convolutional Neural Network, which first appeared in the ImageNet Recognition Challenge. Inceptionv3 was expected to offer deeper networks while still restricting the number of parameters to "approximately 25 million," as opposed to AlexNet's 60 million. The Inceptionv3 architecture has been used in a wide range of computer vision applications and is typically "pre-trained" by ImageNet. One such application is in biological sciences, where it aids in the study of leukemia (Rafiq and Albert, 2022).

4. ResNet50V

ResNet is an abbreviation for Residual Network. This cutting-edge neural network was constructed by Kaiming He, Xiangyu Zhang, and Shaoqing Ren. Res-net50 is a variation capable of running up to 50 neural network layers. The building block was redesigned as a bottleneck design because to worries about the time necessary to train the layers. This time, instead of the previous two levels, a three-layer stack was employed. As a result, the Res-net34's 2-layer bottleneck blocks were replaced with 3-layer bottleneck blocks, yielding the Resnet50 design. This model's accuracy is significantly higher than that of the 34-layer ResNet model(He et al., 2016).

5. DenseNet

DenseNet's layers receive more data from previous layers and give feature maps to subsequent levels. It is known as "concatenation." Each tier benefits from "collective knowledge" provided by the levels above it(Huang et al., 2017)

2.3.2 Support Vector Machine

SVM, or Support Vector Machine, is a common Supervised Learning technique for classification and regression problems. However, it is generally utilized in Machine Learning for categorization problems. The SVM algorithm's purpose is to discover the optimal line or decision boundary for classifying n-dimensional space, so that in the future we may easily insert new data points into the appropriate category. A hyper-plane is the optimal boundary. SVM selects the extreme points/vectors that contribute to the formation of the hyper-plane. The technique is called the Support Vector Machine, and the extreme examples are called support vectors (Shmilovici, 2009).

Linear SVM is used to classify linearly separable data, which implies that if a dataset can be divided into two groups using a single straight line, it is termed linearly separable data and is categorized using the Linear SVM classifier. An example will demonstrate how the Linear SVM algorithm works. Let's say there are two tags (green and blue) and two characteristics, as shown in Figure 2.3. (x1 and x2). We need a classifier that can tell the difference between green and blue coordinate pairs (x1, x2). We may easily draw a straight line to distinguish these two classes because it is a two-dimensional space. However, various lines may be drawn to distinguish these groupings. As a result, the SVM approach assists in the finding of the best decision boundary or line; this best border or area is known as a hyperplane(Huang et al., 2018). In both kinds of lines, the SVM technique finds the nearest point. These are known as support vectors. The margin is defined as the distance between the vectors and the hyper-plane. SVM's purpose is to maximize this margin. The hyperplane with the greatest margin is the best (Huang et al., 2018).
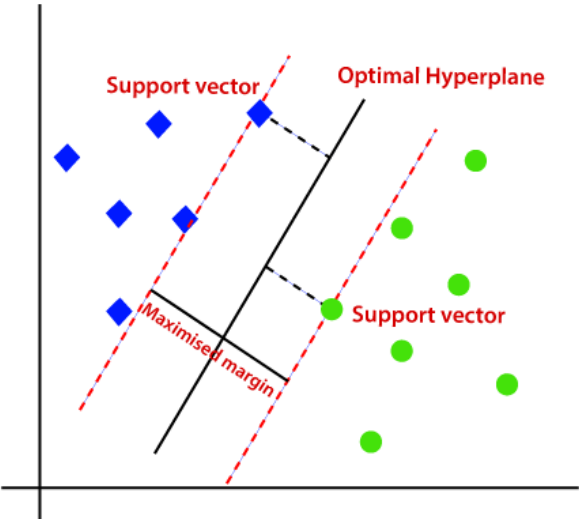
Figure 2. 3 Structure of Linear Support Vector Machine (Huang et al., 2018)

Non-linear SVM classifiers are used to classify non-linearly segregated data, which implies that if a dataset cannot be categorized using a straight line, it is classed as non-linear data and the Non-linear SVM classifier is employed. We can split data that is structured linearly with a single straight line, but we cannot divide data that is not organized linearly. Figure 2.4 shows that we need to add another dimension to differentiate these data values. Two dimensions are utilized for linear data, x and y, so a third will be added for non-linear data (z) (Li et al., 2019a). It may be computed as follows:

$$Z = x2+y2 \ldots\ldots\ldots\ldots\ldots\ldots\ldots\ldots\ldots\ldots\ldots\ldots\ldots\ldots\ldots\ldots\ldots \text{(2.1)}$$

We are in three-dimensional space, and it appears to be a plane parallel to the x-axis. Consider the figure after converting it to 2d space with z=1.
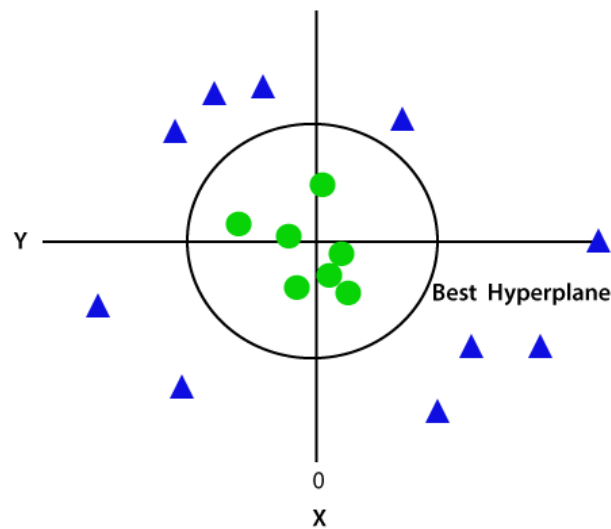
Figure 2. 4 Structure of non-Linear Support Vector Machine(Li et al., 2019a)

2.3.3 K-Nearest Neighbor (KNN)

K-Nearest Neighbor is a key Machine Learning approach that employs the Supervised Learning strategy. The KNN approach assumes similarity between the new case/data and previous cases and allocates the new case to the most analogous category to the existing categories. The KNN approach preserves all past data and classifies new data points based on similarity. This means that anytime fresh data is generated, the KNN approach can quickly categorize it (Guo et al., 2003).

The KNN technique may be used for both regression and classification; however it is more typically employed for classification. As a non-parametric approach, KNN makes no assumptions about the underlying data. It is also known as a lazy learner algorithm since it does not immediately learn from the training dataset; instead, it stores the knowledge and acts on it later while classifying. The KNN approach merely keeps the dataset during the learning phase and then categorizes it into a category that is quite similar to the incoming data(Zhang et al., 2017).

The following stages will demonstrate how the KNN algorithm works: Choose the number K of neighbors in the first stage. The Distance measure be-

tween K neighbors is determined in the second phase, and the K closest neighbors are picked based on that distance. Then, count how many data points are in each category among these k neighbors. Assign the new data points to the category that has the most neighbors. Finally, our model is complete(Zhang et al., 2017).
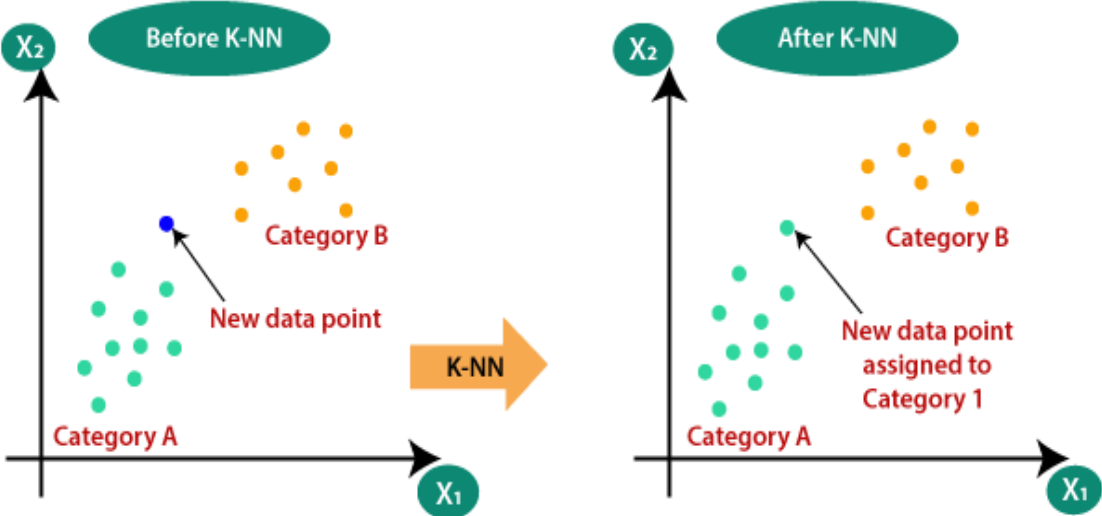

Figure 2. 5 Structure of K-Nearest Neighbor (KNN)

CHAPTER THREE

METHODOLOGY

3.1 INTRODUCTION

Urinalysis is the examination of urine on physical, chemical, and microscopic levels. A series of tests are performed to identify and analyze numerous chemicals that move through the urine. In this chapter, main structure of the proposed approach for classification urine sediment images and used dataset will be explained thoroughly. Explanations are also provided of how data was gathered and analyzed.

In addition, all information and actions linked to data image, the phases of processing and data preparation before recognition were explained, such as (gray scale and threshold operation). This chapter illustrates the methods and structure of all algorithms that are used to perform analyzing urine sediments.

3.2 GENERAL FRAMEWORK OF THIS STUDY

The designed automated urinalysis system includes the following steps: first of all, for this study microscope urine images are gathered in real human urine to create real dataset. After collecting more than thousand images, some preprocess on the images are performed to make them simpler and clearer to achieve accurate and good result.

In the second step of image processing, converting the images to gray scale image and a threshold operation (binarization) are performed. Then, analyzing and classifying images are evaluated and performed in two methods. For the first method convolution neural network and five types of ConvNet model are proposed,

In this method the images directly go to classifying algorithms. But in the second method before going to classifying algorithms feature extraction was performed, extracted 22 features. Lastly, the extract features were introduced to the classifiers to distinguish subjects. In this part of the study, Red blood cells, calcium oxalate crystals, cysten crystals, and uric acid crystals are the objective classes. The automated microscopic urinalysis work is provided a urine specimen with up to a few hundred pictures of analysis so that it can categorize each analysis. Figure 3.1 and Figure 3.2 shows a flowchart that demonstrates the basic features of the proposed (urinalysis) system.

In terms of classification, eight different algorithms have been employed, including Convolution Neural Network, five type of transfer learning algorithms such as (MobailNet, VGG16, Inception v3, DenseNet, ResetNet), Support Vector Machine and k-nearest neighbors. The highest accuracy rate by MobailNet has been achieved among the other classifiers also other four types of transfer learning algorithms and our proposed CNN has achieved the best result. All eight algorithms by assigning real dataset as the training set and testing set have been applied.
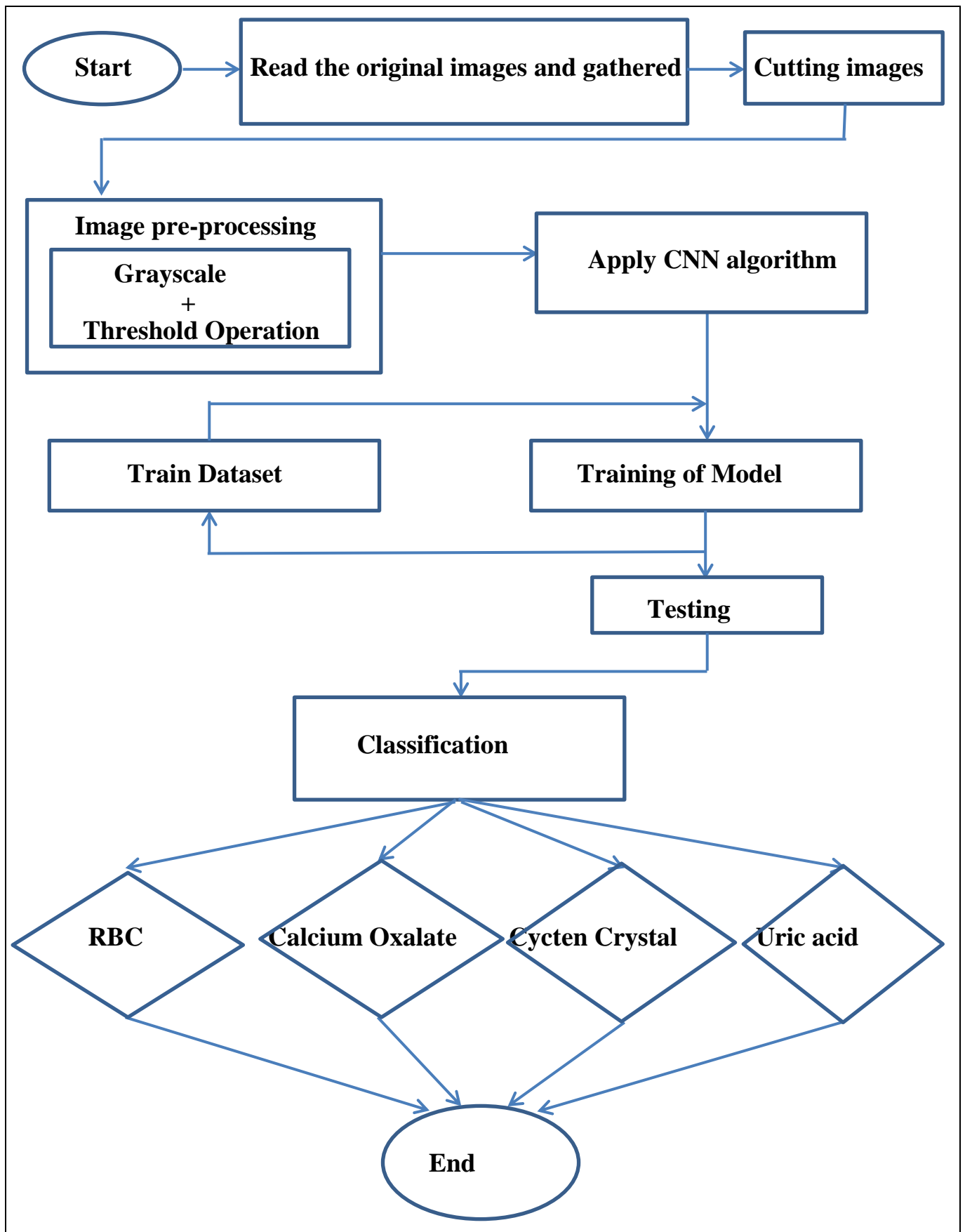
**Figure 3. 1** The general framework of the first proposed method
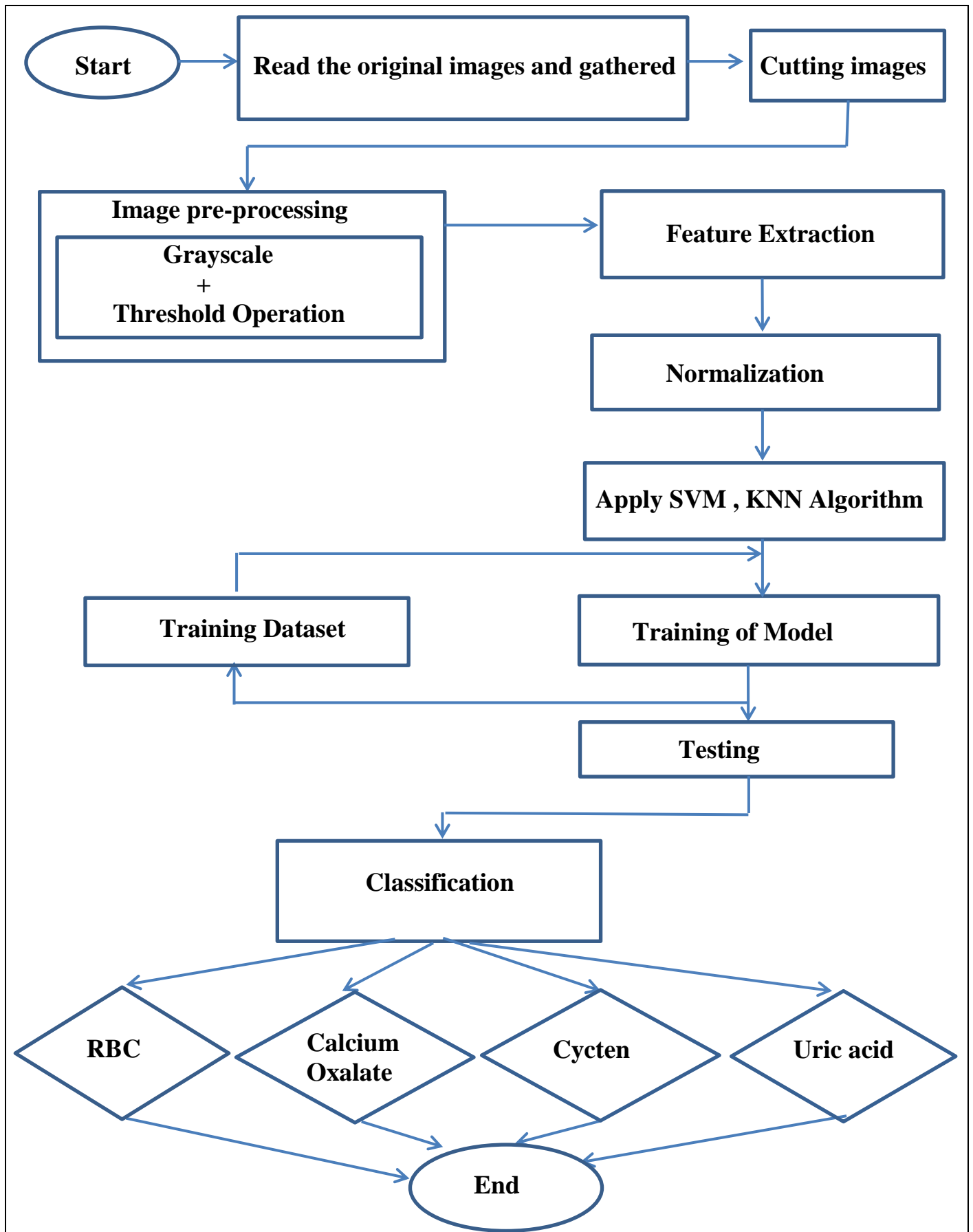
Figure 3. 2 The general framework of the second method

3.3 DATA COLLECTION

For this study, a real dataset was prepared, the images gather of particles found were in microscopic urinalysis. Microscopic images of urine sediments are manually collected from the Shorsh Provincial People's Hospital in Sulay-maniyah city and Shifa Privet Laboratory in Ranya city during three months in 2021. To produce a real urine sediment dataset, images were taken from real human urine using a microscope with 4x and 10x magnifiers. These two labora-tories gathered 1,420 urine sediment images in total. After the removal of many images with noise, there are 820 images left shown in Table 3.1. Mainly in this study four types of urine sediment images are focused on such as: Red Bleed Cell (RBC) and three types of Crystals (Oxalate, Cysteine, Uric acid). Some samples are displayed in Figure 3.3

Table 3. 1 Dataset

.

Urine Sediment	Number of Images
Red Blood Cell	231
Calcium Oxalate	228
Cysteine Crystal	102
Uric acid Crystal	259
Total	**820**
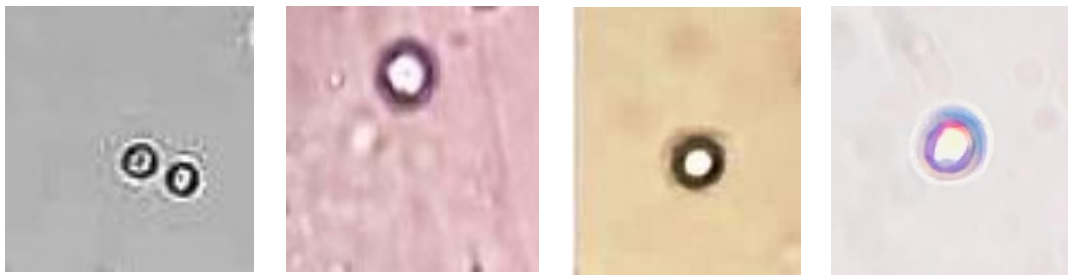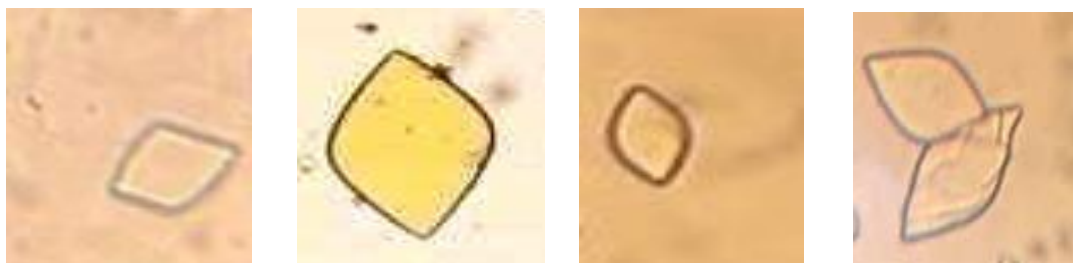
Figure 3. 3 Examples of urinary sediment: a) RBC, b) Calcium oxalate crystal, c) Cystine crystal, d) Uric acid crystal.

3.4 GRAYSCALE AND THRESHOLD OPERATION

The original urine microscopic image is frequently degraded by noise, thus it must be preprocessed in order to offer more precise information about the edge. First and foremost, transform the RGB color image to a grayscale image. This is done for a variety of reasons, including (Color complexity, Easier visualization, Noise reduction, Code complexity, Speed) the RGB type have a lot of information that may or may not be needed for particular processing. When convert an RGB image to grayscale, lose a lot of information that is not needed for processing. In the case of an RGB scale image, each component has a separate intensity label R,G,B. Three channels make up an RGB image. Each channel typically consists of 8 bits. As a result, for a color image there is a large amount of data to store and/or modify(Zheng et al., 2010).

In addition, a threshold operation is conducted in the other preprocessing phase. Image thresholding binarizes images based on pixel intensities; usually, a gray scale image and a threshold are used as input to such thresholding algorithms. The final product is a dual image.

If an input pixel's intensity exceeds a threshold, the associated output pixel location is marked black (foreground), and if the intensity of the input pixel is less than or equal to the threshold, the output pixel position is marked white (background)(Mahmoud and Marshall, 2008). This conversion provides simplicity when applying any operation in image enhancement as shown in Figure 3.4.

Image thresholding is utilized as a pre-processing step in various applications. For instance, it might be used in medical image processing to detect a tumor in a mammography(Kekre et al., 2009) or to locate a natural catastrophe in satellite images(Nair and Bindhu, 2016).

Figure 3. 4 The urine sediment images after converting to grayscale and performing Threshold operation

3.5 PROPOSED MODELS OF CLASSIFICATION

In the other step of this work after preparing images machine learning and deep learning algorithms are used to classified urine sediment images. For the classification performed two methods:

3.5.1 METHOD 1:

In the first method in this study, the images directly go to classifying algorithms. After making some pre-process on the images to make them simpler and clearer, the dataset of images goes to scanning by classifiers. Following the successful preprocessing of images, the datasets were divided into training and testing sets. The training set received 80% of the dataset while the testing set received 20%. For the classifiers CNN model and five type of transfer learning model ware proposed.

3.5.1.1 Proposed Model Based On Convolution Neural Network

The designed network of CNN architecture consists of five convolution layers, the size of each convolution kernel in the convolution layer is 3×3. As well as after each convolution layer has a Maxpooling layer pooling window size is 2×2. As well as train the dataset more time in the other window size, get best result in the kernel 3×3 and for Maxpooling layer is 2×2. The convolutional and

pooling layers of the CNN extract features, while the connected layer trans-forms the gathered features into the final output. Nonlinear and linear processes, such as the activation function and the convolution operation, are frequently used in the convolution layer. Convolution, a linear operation, is used to extract features, and the outputs are then treated by a nonlinear activation function to improve feature extraction.

By conducting down sampling, the pooling layer was able to minimize the number of input parameters and the dimensionality of the feature maps. The results are then routed via a nonlinear activation function to improve feature extraction. The rectified linear unit is the activation function (ReLU). And the network's final output was mapped utilizing three completely connected layers. Finally, the Softmax activation functions are applied to the last connected layer, and the Softmax is input layers to categorize and identify the cell feature. In the model used learning rate 0.001with the batch size of 32 for 500 epochs. The number of batch size is chosen based on the same idea of the number of filters. The model trained from 1 epoch until 500 increased by 1 in each test.
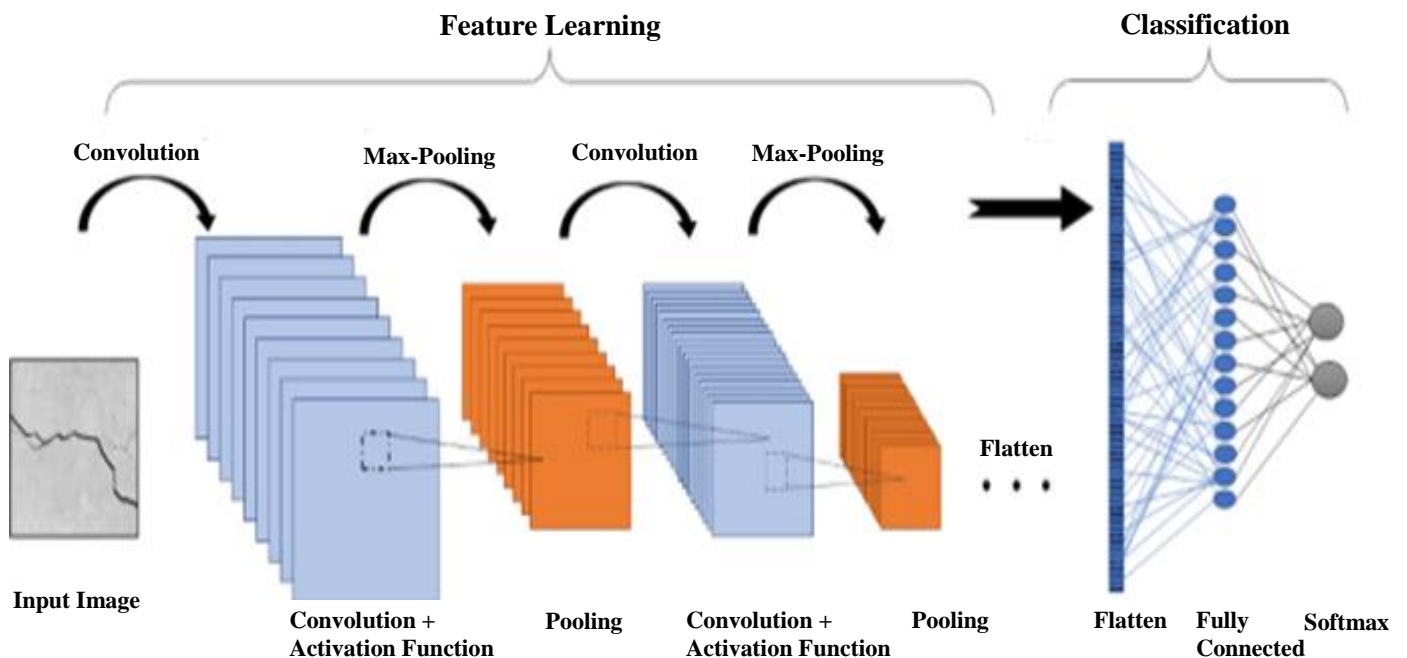
Figure 3. 5 Proposed CNN Network

3.5.2 METHOD 2:

After collecting images and making pre-process on them, features extraction is performed. Extract 22 features from each image. Prepared numeric dataset consists of 820 rows as mentioned and for this study there are 820 images each row represents an image. Also the dataset consists of 23 columns, each column represents a feature of image, and last column is a label.

3.5.2.1 Feature Extraction

Feature extraction is a dimension reduction technique that divides a big amount of raw data into smaller processing sets. These huge data sets contain a large number of variables that need a significant amount of computer resources to process. The practice of merging variables into features in order to decrease the quantity of data that must be processed while still comprehensively and pre-cisely identifying the initial dataset is known as feature extraction. Feature ex-traction is useful when need to decrease the amount of resources required for processing without losing any important or meaningful information. It may also reduce the quantity of duplicated data for a specific study. Furthermore, feature extraction can contribute to additional benefits such as improving accuracy, lowering the risk of overfitting (Overfitting happens when a model learns the in-tricacies and noises in the training set to the point where the model's efficiency on unknown data suffers), boosting up in the training set, and improving data visualization.(Mohamad et al., 2015).

The statistical features namely means, standard deviation, variance, kurtosis (only for Hold Time) and skewness (only for Hold Time) have been extracted for each computed keyboard dynamics of Hold Time, Flight Time, Press Laten-cy, Release Latency, Dash and Triple in this study, which are all 21 features in-cluding the typing speed feature. Their explanations and equations have written below.

Mean: is a metric for central tendency. It is a single number that seeks to indicate a set of data by recognizing the center of that group of data. Measurements of central tendency are also referred to as measures of central placement. They're also known as summary statistics. The most likely measure of central tendency is the mean (also known as the average), which is the most common and well-known measure of central tendency and may be used with both continuous and discrete data. Equation represents the mean formula (3.1) (Ball et al., 2020)

$$\text{Mean} = \frac{\sum X_i}{n}$$ ……………………………………………. (3.1)

Variance: is the measurement of the spread among numbers in the dataset. The value of variance is found by calculating the contrast between the mean and each number in the data set, to have positive values it should be squared, and at the end dividing the summation of all the squared values in excess of the number of values in the data collection. The Equation (3.2) shows the calculation (Ball et al., 2020).

$$Variance\ (\sigma^2) = \frac{\sum_{i=n}(X_i - \overline{X})^2}{n}$$ …………………….………. (3.2)

Standard Deviationis a statistic that assesses a dataset's dispersion relative to its mean. It is calculated as the square root of variance by determining the difference between each data point and the mean. The larger the standard deviation, the more spread out the data, since if the data points are further from the mean, there is a bigger variation within the data set, as shown in Equation below (3.3) (Ball et al., 2020).

$$\text{Standard Deviation}\ (\sigma) = \sqrt{\frac{\sum_i {}^n (X_i - \overline{X})^2}{n}}$$ …………………. (3.3)

Skewness: is commonly described as a measure of the symmetry or lack of symmetry of a dataset. A full symmetrical data set has a skewness of 0, if the distribution of the data sets is normal. Equation (3.4) illustrates the skewness (Ball et al., 2020).

$$\text{Skewness} = \frac{n}{(n-1)(n-2)} \sum \frac{(xi - \bar{x})^3}{s^3} \dots\dots\dots\dots\dots\dots\dots\dots\dots\dots (3.4)$$

Kurtosis: is a numerical measure used to define the degree to which scores cluster in the tails, or the peak of a frequency distribution is called Kurtosis. The tallest part of the distribution is the peak, and the ends of the distribution are the tails. In other words, it may be claimed that Kurtosis informs us practically nothing about the peak's shape; its sole unambiguous interpretation is in terms of tail extremity, Equation (3.5) shows the kurtosis (Ball et al., 2020).

$$\text{Kurtosis} = \left\{ \frac{n(n+1)}{(n-1)(n-2)(n-3)} \sum \frac{(xi - \bar{x})^3}{s^3} \right\} - \frac{3(n-1)^2}{(n-2)(n-3)} \dots\dots\dots\dots\dots\dots (3.5)$$

Because many machine learning algorithms aim to discover trends in data by comparing features of data points, by applying normalization using Mini-Max Normalization after feature extract on images and prepare dataset. When the features are on significantly different scales, however, there is a problem.

3.5.2.2 Normalization

Normalization is the process of adjusting the scale of all data points so that each attribute has the same weight. The phrases standardize and normalize are synonymous in data pre-processing, but the later term has different statistical connotations). Min-max normalization is one of the most often used data nor-malizing algorithms. The lowest value for each characteristic is set to zero, the highest value is set to one, and all other values are set to a decimal between Ze-

ro and one. Changing the measuring units for height and weight, such as meters to inches or kilograms to pounds, can have a significant influence on the results. In general, expressing a characteristic in smaller units results in a bigger value ring and, as a result, a stronger effect or "weight" for that quality.

The goal of normalizing data is to equalize the weight of all qualities. Normalization is highly beneficial in algorithms that employ neural networks or distance measurements, such as nearest-neighbor classification, prediction, and clustering. Normalizing the input values for each attribute measured in the training tuples can assist speed up the learning stage when utilizing the neural network feedforward technique for classification processing.

Normalization of data may be achieved in a variety of ways. It investigates min-max normalizing, z-score normalizing, and decimal scaling normalization. For our purposes, let A be a number attribute with n observed values, v1, v2...vn.

Min-max normalization= (Value-Min) / (Max-Min) .... (3.6)

3.5.2.3 Apply the Training Algorithms

1. Support Vector Machine (SVM)

SVM is a well-known Supervised Learning approach that is used to solve classification and regression problems. However, it is largely used in Machine Learning for classification difficulties (Shetty and Rao, 2016).

The goal of the SVM approach is to determine the best line or decision boundary for classifying n-dimensional space, so easily place new data points are simply put in the appropriate category in the future. In this study SVM was used to classify multiclass (RBC, Calcium Oxalate, Uric acid, Cyctine Cristal). After pre-processing and normalizing the dataset, after successfully preprocessing the images, the datasets were separated into two groups: training and testing. The training set got 80% of the dataset, whereas the testing set got 20%.

Finally, the SVM classifier was trained using the training data. To attain the best results, the model performance may be tweaked by adjusting the values of C (Regularization factor), gamma, and kernel. The effectiveness of any produced software or algorithm is critical. As a result, the performance of the models was tested and compared using measures such as accuracy, recall, precision, and F1 score. The confusion matrix was also computed.

2. K-Nearest Neighbors (KNN)

The Supervised Learning methodology is used in the fundamental Machine Learning method of k-nearest neighbors. The KNN approach keeps all previous data and uses similarity to classify new data points. This means that as fresh data is created, the KNN technique can categorize it quickly. This implies that the KNN method assumes similarity between the new case/data and earlier cases and assigns the new case to the category with the greatest resemblance to the existing categories(Zhang et al., 2017).

The dataset was separated into training and testing sets after it was pre-processed and standardized. The KNN classifier was then trained on the training data. Model In the experiment, cross validation with ten validations and stratified sampling were used. The k value (nearest neighbor threshold) was changed to acquire the best results. Using k= 5 was the optimal choice that resulted in the highest accuracy, recall, and precision rates.

3.9 PERFORMANCE EVALUATION

Empirical studies have shown that each metric has precise specifications that measure several aspects of the algorithms being estimated, which makes it hard to choose which metric is suitable to use for different problems. Because of the huge weighted disparities that frequently exist between the actual and projected values, it is often difficult to identify which measures are appropriate for evaluating algorithms in clinical care. Machine learning algorithms' success is evaluated based on prediction accuracy, which is frequently inadequate in the event

of unbalanced data, and mistake costs differ dramatically.

Machine learning performance assessments include the amount of trade-off between negative and positive true rate, as well as precision and recall. Precision, recall, and F-Measure are three performance metrics for information extraction. The performance of any machine learning model is determined by metrics such as True Positive Rate, False Positive Rate, True Negative Rate, and False Negative Rate. The genuine negative rate or negative class accuracy is used to calculate specificity. The sensitivity is also known as the genuine positive rate or positive class precision. In general, they are both utilized to diagnose clinical testing(Danjuma, 2015).

Accuracy: provides the proportion of the total number of correct estimations made by the classifiers, regardless of whether the predictions are negative or positive. It is formulated as illustrated in the Equation (3.7) (Danjuma, 2015) .

$$Accuracy = \frac{TP + TN}{TP + TN + FP + FN} \ 100 \ \%$$ …………………….…..……. (3.7)

Sensitivity (so-called Recall): is an estimate of the number of definite positive instances projected to be positive (or true positive). This indicates that an additional proportion of certain positive instances will be projected as negative (and, therefore, could also be labeled as the false negative). This can also be expressed as a false negative rate. The amount of people suffering from the disease who correctly predicted as the ones suffering from the disease is sensitivity. Another explanation is that unhealthy people were predicted correctly (Danjuma, 2015). The equation of sensitivity has been written in Equation (3.8):

$$Sensitivity \ (Recall) = \frac{TP}{TP + FN} \ 100 \ \%$$ …………………………. (3.8)

Precision: The positive predictive value is the number of correct positive predictions divided by the total number of positive predictions. It is also known as positive predictive value (PPV), with 1.0 being the highest precision and 0.0 being the lowest. Precision is defined as the number of accurate answers divided by the total number of correct responses (TP + FP). Precision is calculated by dividing the total number of properly categorized positives by the precision value, where higher precision indicates a greater number of positives or a smaller number of FP (Kabir, 2019) as its shown in Equation (3.9):

$$\text{Precision} = \frac{\text{TP}}{\text{TP + FP}} \quad \dots\dots\dots\dots\dots\dots\dots\dots\dots\dots\dots\dots\dots\dots\dots\dots\dots\dots\dots \ (3.9)$$

F-Measure: is the arithmetic mean of the genuine positive rate (recall) and accuracy. It is challenging to compare two models with great accuracy but low recall. It employs harmonic mean instead of 28 arithmetic mean, penalizing extreme values more severely. As a result, F-Measure is always closer to the lower precision or recall value (Kabir, 2019) as its shown in Equation (3.10) :

$$\text{F} - \text{measure} = 2 * \frac{\text{Recall} * \text{Precision}}{\text{Recall} + \text{Precision}} \quad \dots\dots\dots\dots\dots\dots\dots\dots\dots\dots\dots\dots\dots\dots\dots \ (3.10)$$

CHAPTER FOUR

EXPERIMENTS AND RESULTS

4.1 INTRODUCTION

This chapter covers the experimental procedures and research outcomes that were employed to support the research strategy.

Clinical test results include limitations, such as the frequency of monitoring and the difficulty of evaluation. As a result, there are unmet medical needs for quantitative and reliable tests that might complete clinical scales for a variety of objectives, including such medication response analysis and recognizing risk groups, among others. This study approach may achieve these values and enable for the objective and regular identification of motor indications of urine analysis. The approach used in this study gives certainty and can accurately differentiate patients to urine analysis to determined kidney stone or urine track infection.

This chapter discusses the experimental methodologies and study findings that support the research strategy. The empirical findings are provided and many simulations have been run in order to find the best method to perform as the classifier.

4.2 SIMULATION TECHNIQUES AND TOOLS

The practical work is the primary mission of this study. For this purpose, a Technique is proposed and built by using, PYCHARM for converting images to grayscale and threshold operation, PYTHON 3.8.5. for analyzing classification results, which is open-source software for classification and using MATLAB(R2014b) So for feature extraction. The evaluate were performed in an Intel Core i7- 8700 CPU 3.20 GHz, 32.0GB, process workstation with NVIDIA GeForce GTX 1660.

4.3 EVALUATION RESULTS

In this study, eight different machine learning models were developed to categorize urine sediment images. The discriminating performance of all eight classification algorithms is shown in Table 4.1 and Figure 4.1 a Models are considered in terms of Accuracy, Precision, Recall, and F1-Score

Table 4. 1 The performance of all classifiers that used in this study

Classifiers Name	Accuracy	Precision	Recall	F1-Score
Proposed CNN model	0.9629	0.9648	0.9575	0.9609
ConvNet (MobileNet)	0.9833	0.9859	0.9722	0.9781
ConvNet (VGG16)	0.9600	0.9635	0.9557	0.9607
ConvNet (InceptionV3)	0.9750	1.0000	0.8889	0.9412
ConvNet (ResNet50V)	0.9606	0.9645	0.9509	0.9607
ConvNet (DenseNet)	0.9750	1.0000	0.8889	0.9412
SVM	0.8902	1.00	0.91	0.95
KNN	0.87	0.91	0.83	0.87
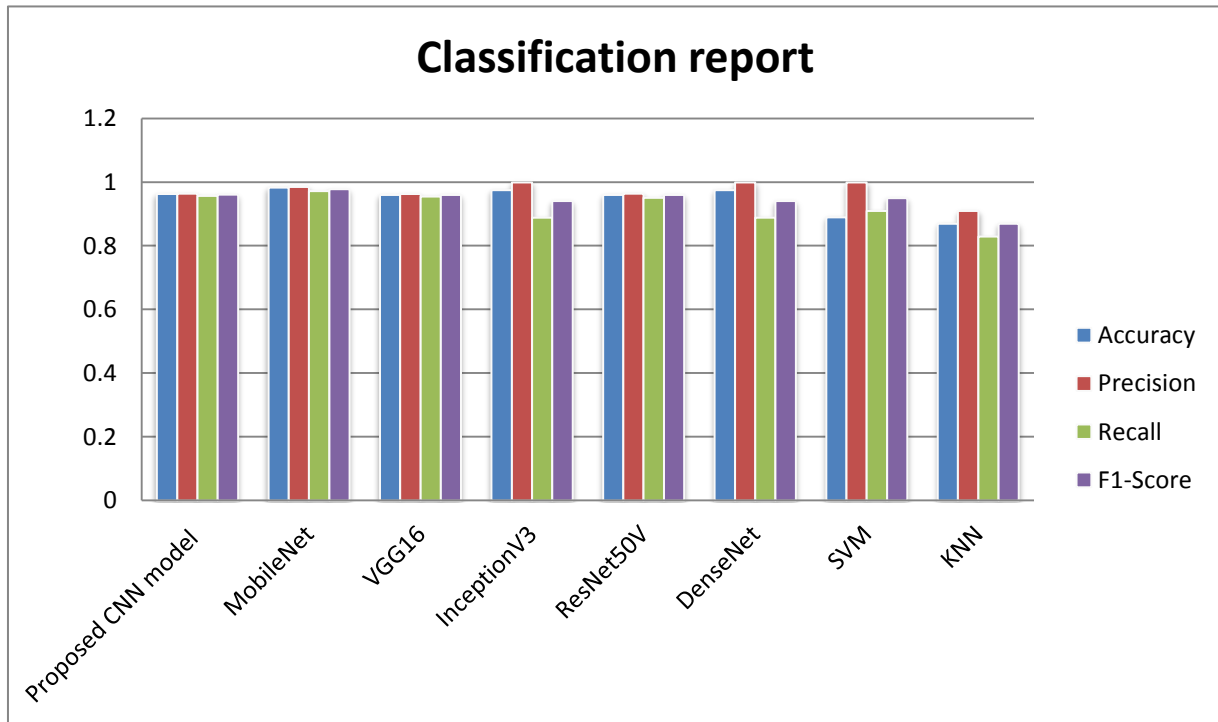
Figure 4. 1 performance result comparison between eight models

4.4 CONFUSION MATRIX

A confusion matrix is a table that is used to analyze the accuracy of classification models on a set of test dates, allowing the performance of an algorithm to be depicted. Classification precision alone may be deceiving. Calculating a confusion matrix may assist in determining what the categorization system performs well and where it fails. The confusion matrix not only reveals the types and counts of mistakes created by the classifier, but also the types and counts of errors produced.

The performance of the best classifier models (MobileNet, InceptionV3, DenseNet, and Proposed CNN model) has been illustrated by the Confusion Matrix in Figure 4.2, Figure 4.3, Figure 4.4 and Figure 4.5. The confusion matrix for all eight algorithms has been explained in Table 4.2.

Each row of the confusion matrix denotes a predicted class instance. The occurrences of the real class are represented by each column of the confusion matrix.

The Confusion Matrix for the best model that is MobileNet shown in Figure 4.2, illustrate the first column in the first row shows cysten class. The classification has been made out of 18 samples in the test dataset, 16 samples which have actually been recognized as a cysten class, this means the true positive for cysteine class is 16 samples among 18 samples. As well as, it made out error in two samples this means there are two false positive. So the second column in the second row shows Oxalate crystal class. The classification was conducted using 33 samples in the test dataset, and all 33 samples were identified as Oxalate crystal class, implying that the true positive for Oxalate crystal class is 33 samples. Therefore, the third column in the third row indicates RBC class; the classification was done using 35 samples in the test dataset, and all 35 samples were identified as RBC class; so, the true positive for RBC class is 34 samples. The last column in the last row indicates the Uric Acid class; the classification was done using 34 samples in the test dataset, and all 34 samples were identified as belonging to the Uric Acid class; this means that the true positive for Uric Acid class is 34 samples.
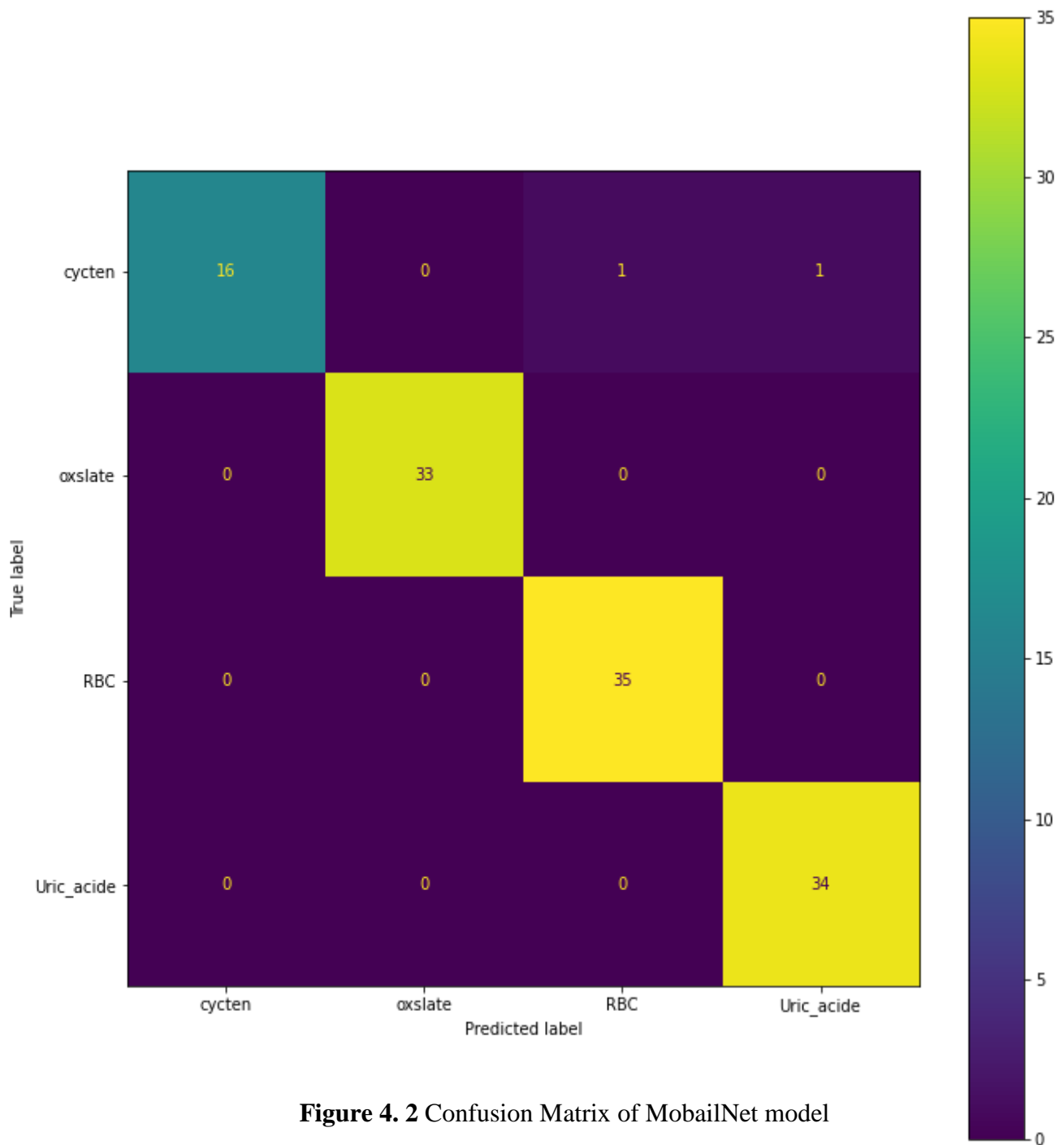
Figure 4. 2 Confusion Matrix of MobailNet model
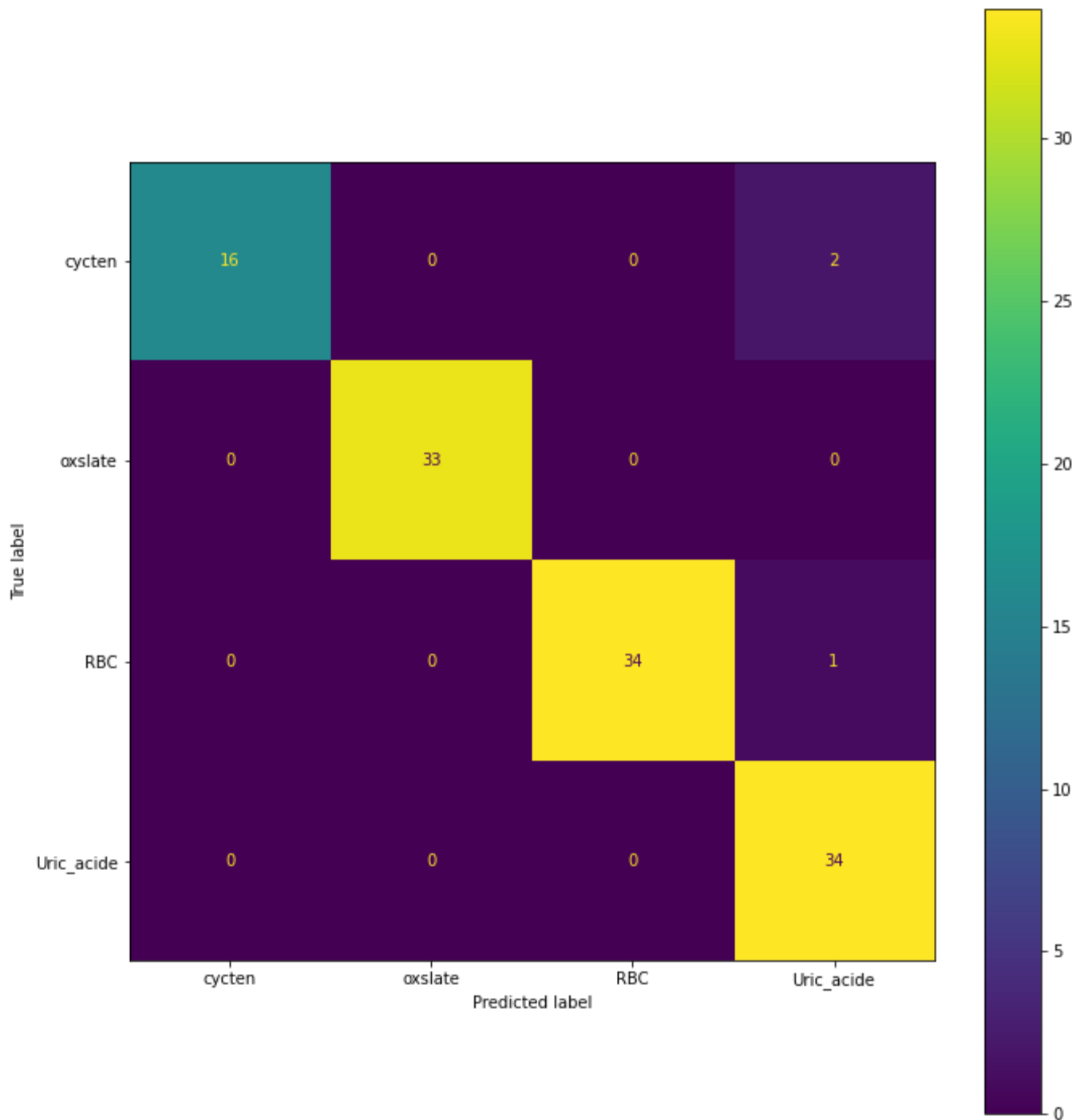
Figure 4. 3 Confusion matrix of the InceptionV3 Model
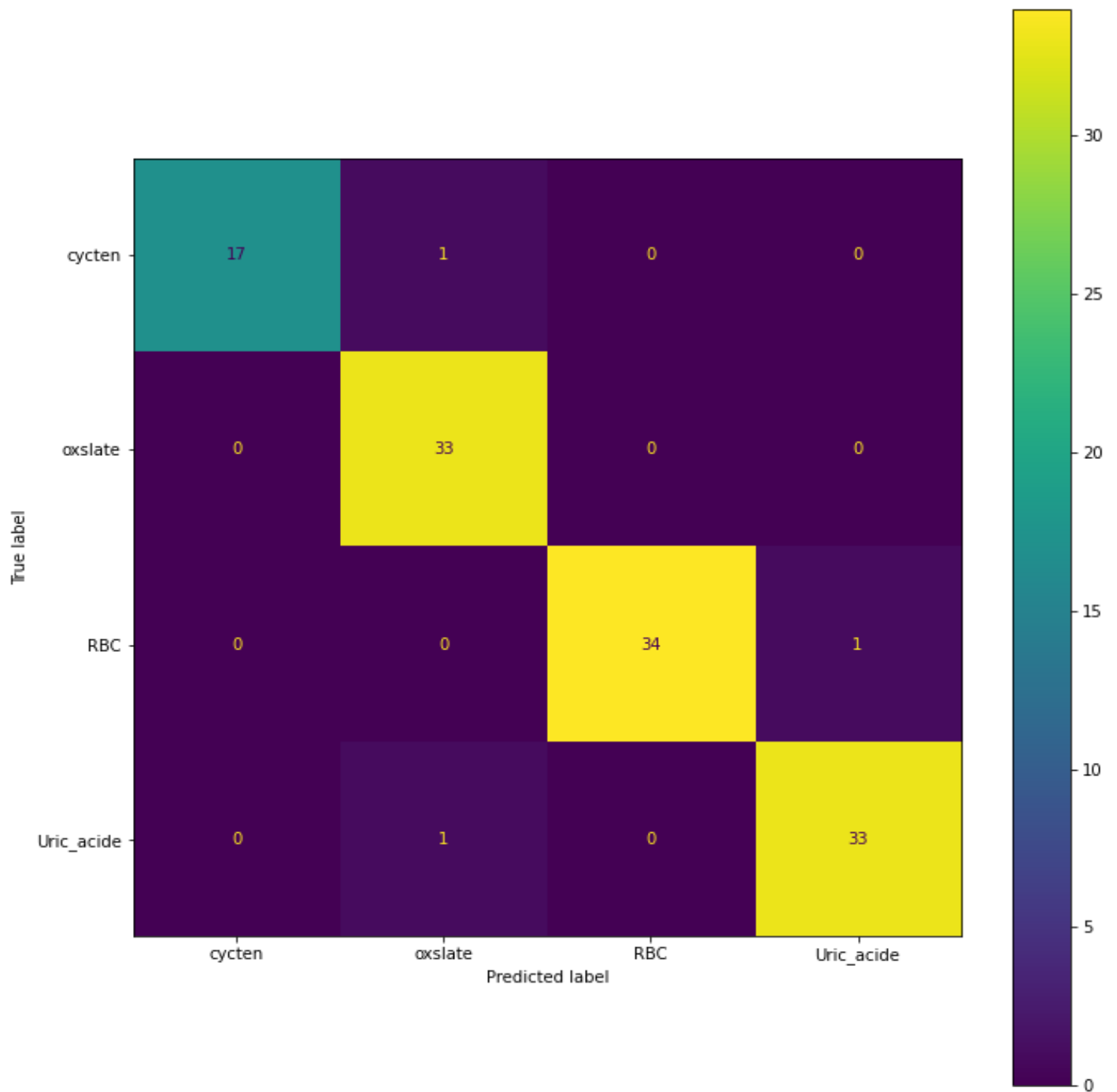
Figure 4. 4 Confusion matrix of the DenseNet Model
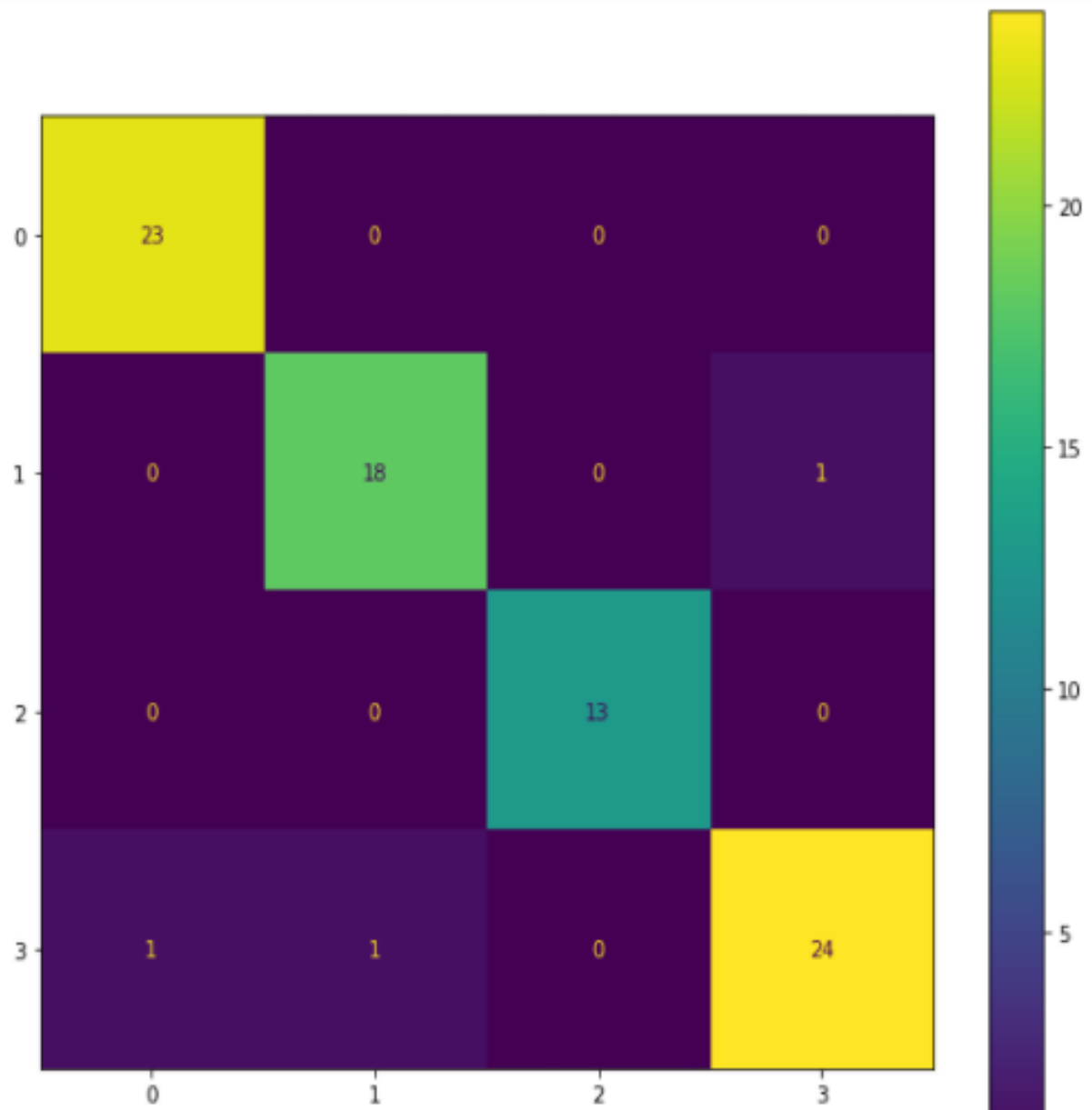
Figure 4. 5 Confusion matrix of the Proposed CNN Model

Table 4. 2 The Confusion Matrix of all eight classifiers.

Classifiers Name	Confusion Matrix				Samples
Proposed CNN model	23	0	0	0	23
	0	18	0	1	19
	0	0	13	0	13
	1	1	0	24	26
MobileNet	16	0	1	1	18
	0	33	0	0	33
	0	0	35	0	35
	0	0	0	34	34
VGG16	16	0	0	2	18
	0	33	0	0	33
	0	0	34	1	35
	1	0	0	33	34
InceptionV3	16	0	0	2	18
	0	33	0	0	33
	0	0	34	1	35
	0	0	0	34	34
ResNet50V	16	0	0	2	18
	0	33	0	0	33
	1	0	33	1	35
	0	0	0	34	34

DenseNet						
	17	0	0	1		18
	0	33	0	0		33
	0	0	34	1		35
	0	1	0	33		34
SVM						
	10	1	0	0		11
	0	21	2	0		23
	0	1	21	3		25
	0	0	2	21		23
KNN						
	10	2	0	0		12
	1	14	1	2		18
	0	2	23	3		28
	0	0	0	24		24

4.5 ACCURACY AND LOSS CURVE

A learning curve is a line that depicts how the learning performance of a model varies over time or with experience. Learning curves are a common diagnostic tool in machine learning for algorithms that learn progressively from a train dataset. Examining model learning curves during training can aid in the detection of learning problems such as an underfit or overfit model. The accuracy curve compares model predictions to actual values in percentage terms to see how well our model predicts. Loss is a monetary value that indicates the total number of mistakes in our model. It assesses how effectively (or poorly) our model is doing. If the errors are substantial, indicating that the model did not perform well, the loss will be considered. Otherwise, our model performs better when the value is smaller.

In Figures 4.6 and 4.7, the accuracy and loss curve of MobailNet model is plotted across the training and validation process. Over different epochs on the real prepared dataset was plotted.

During the training phase, Figures 4.6 show the accuracy curve of MobailNet model. Training accuracy curve shows that accuracy increased from 48.54% at the first epoch to 98.27% at the end epoch. Validation accuracy curve shows that accuracy enhanced from 62.43% at the first epoch to 97.83% at the end epoch. Also the training loss curve shows in Figure 4.7 that loss decreased from 12.38% at the first epoch to 0.1% at the end epoch. Validation loss curve shows that loss decreased from 11.14% at the first epoch to 0.4% at the end epoch. Also in all other models it can be seen in next Figures the accuracy curve increased and the loss curve was decreased.

Figure 4. 6 Accuracy curve across the training and validation process for MobailNet Model

Figure 4. 7 Loss curve across the training and validation process for MobailNet Model

Figure 4. 8 Accuracy curve across the training and validation process for Inception v3 Model

\

Figure 4. 9 Loss curve across the training and validation process for Inception v3 Model

Figure 4. 10 Accuracy curve across the training and validation process for DenseNet Model

Figure 4. 11 Loss curve across the training and validation process for DenseNet Model

Figure 4. 12 Accuracy curve across the training and validation process for VGG16 Model

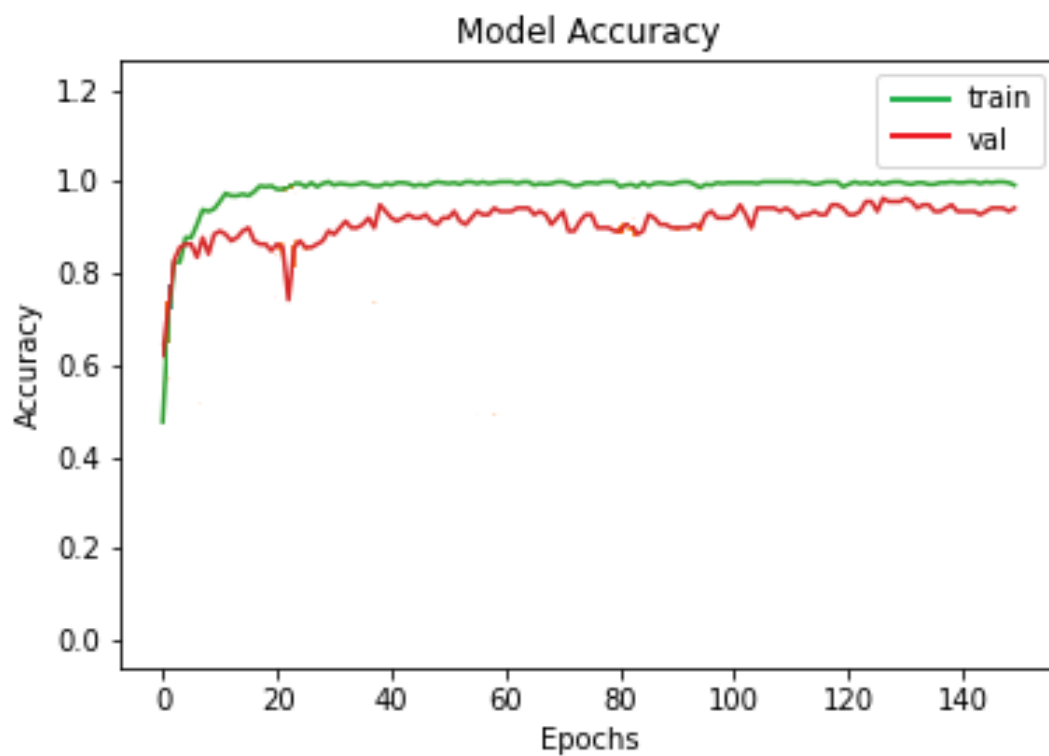**Figure 4. 13** Loss curve across the training and validation process for VGG16 Model
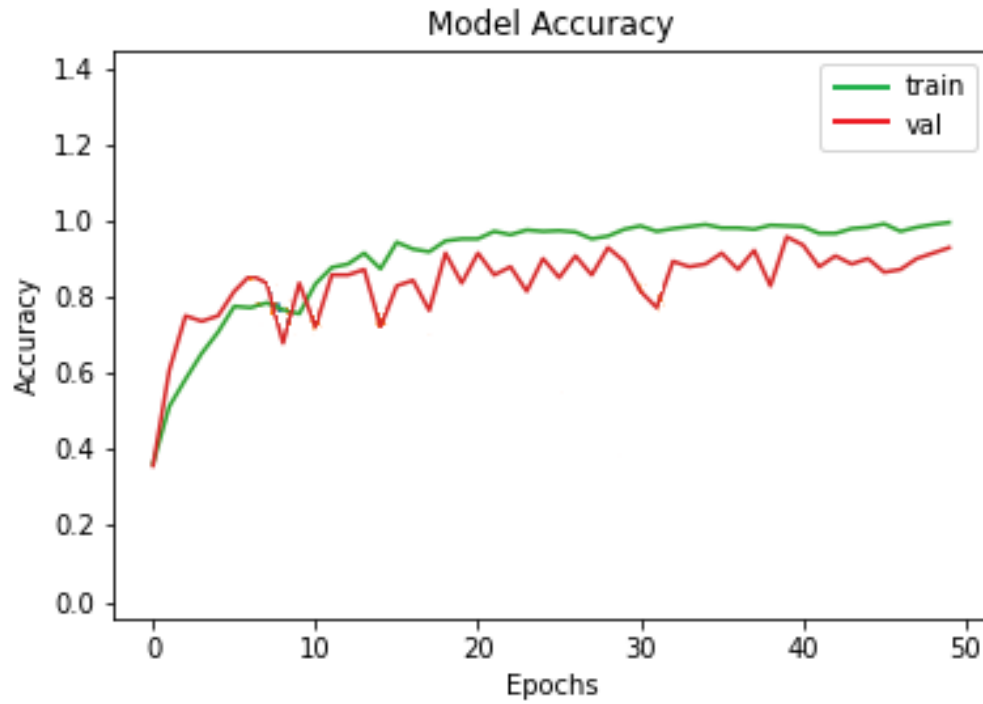
Figure 4. 14 Accuracy curve across the training and validation process for ResNet50 Model

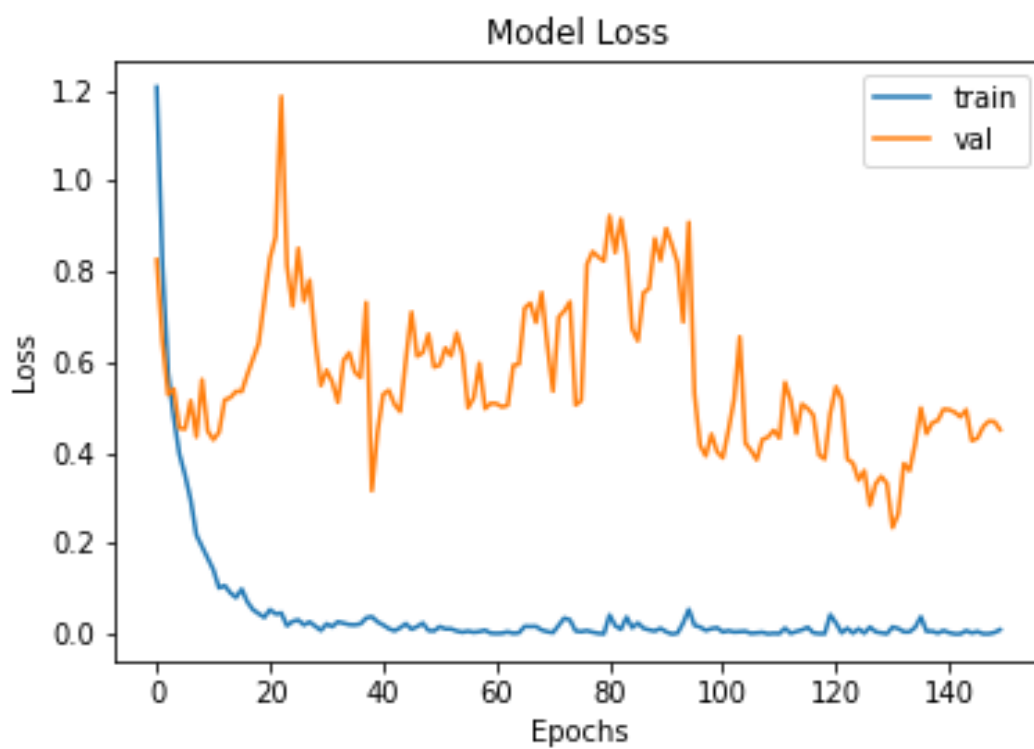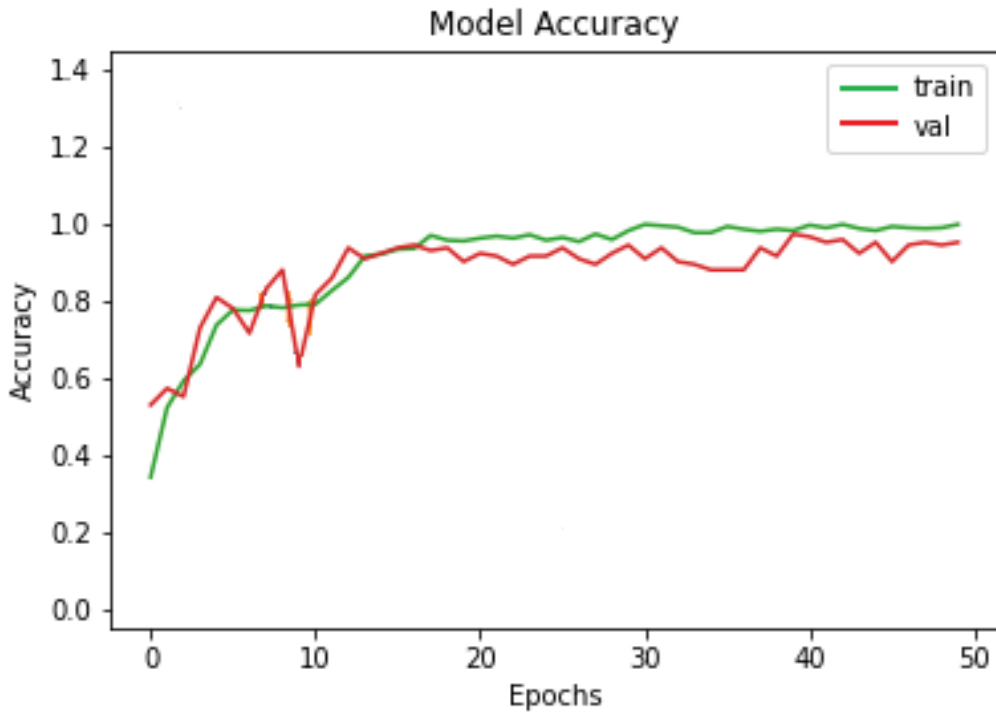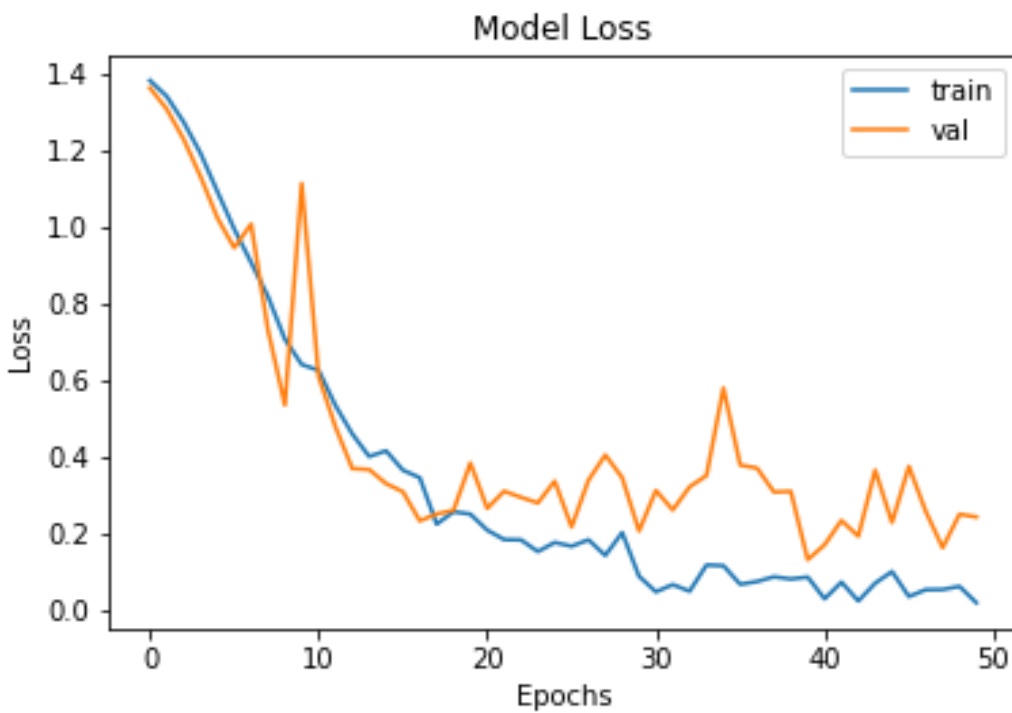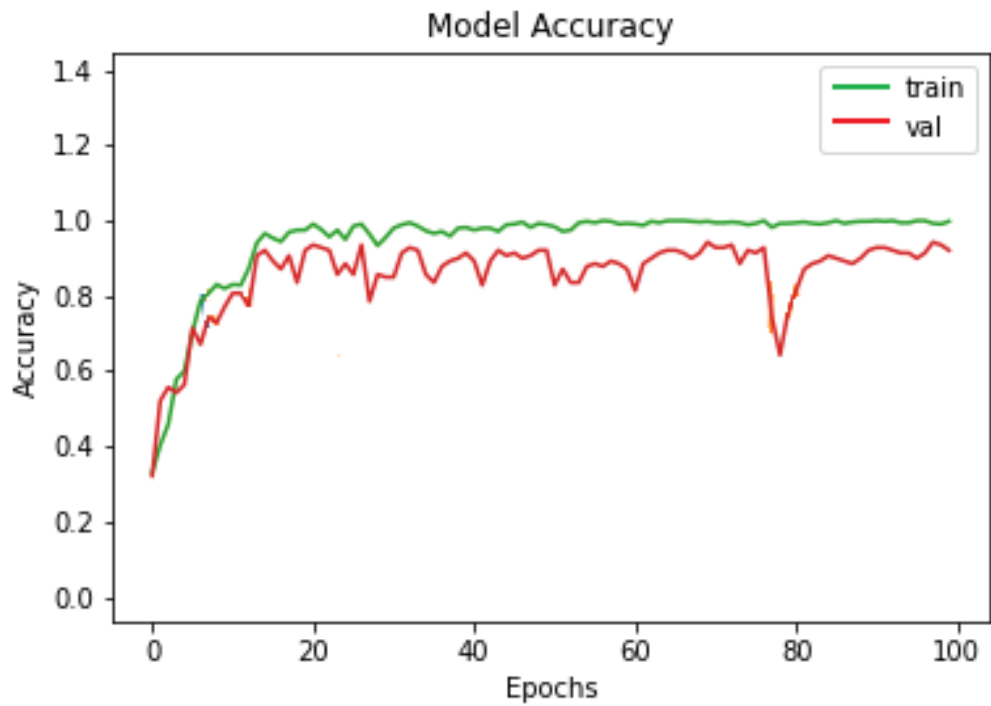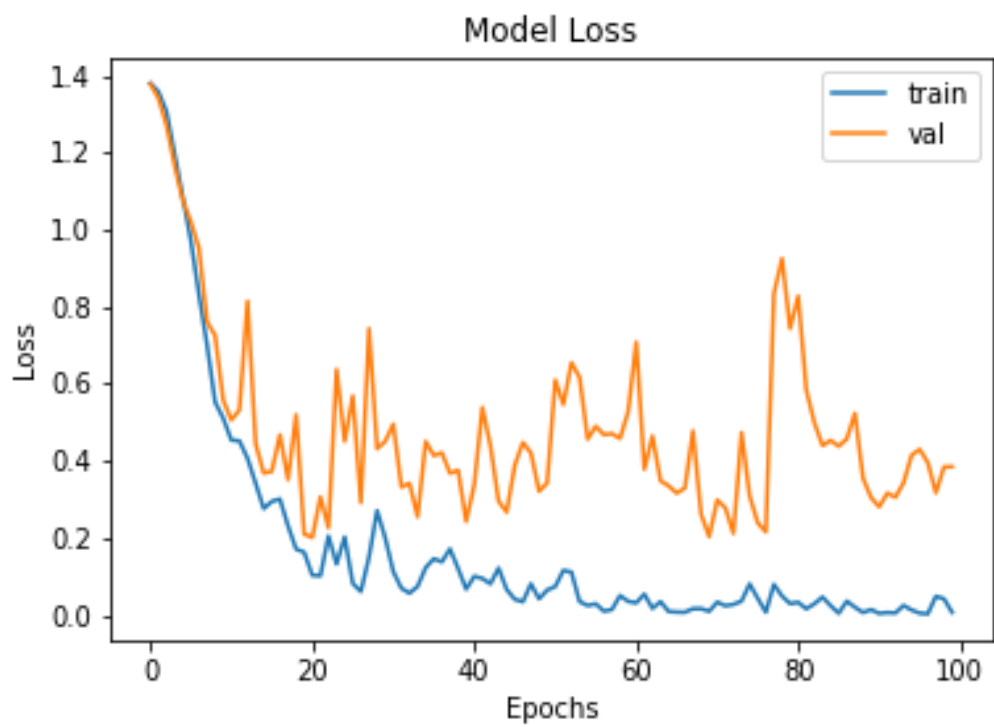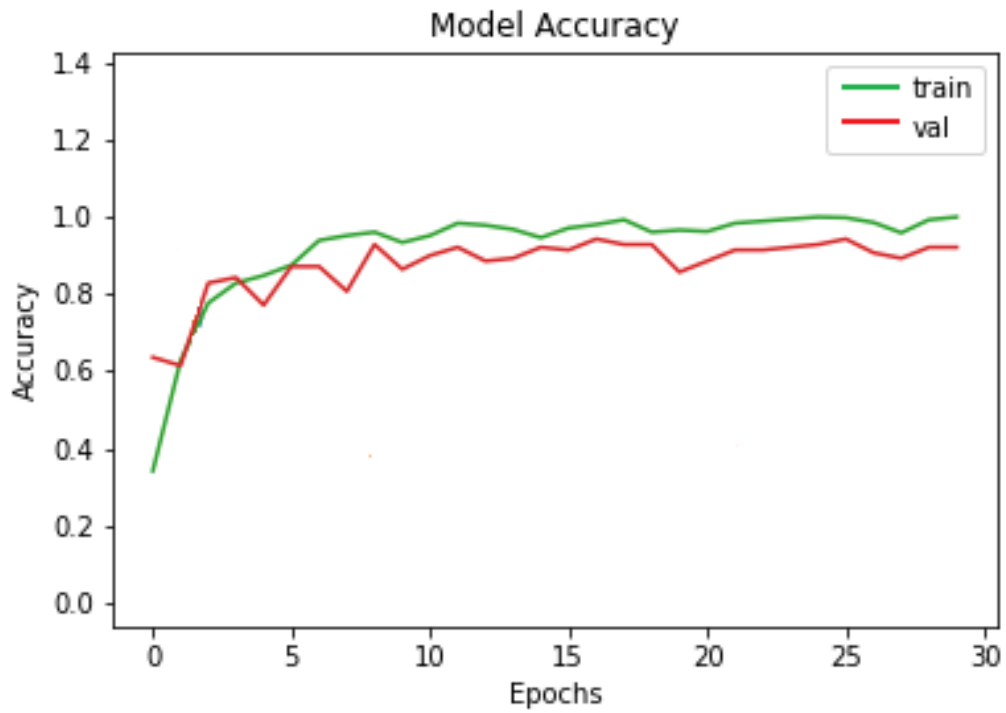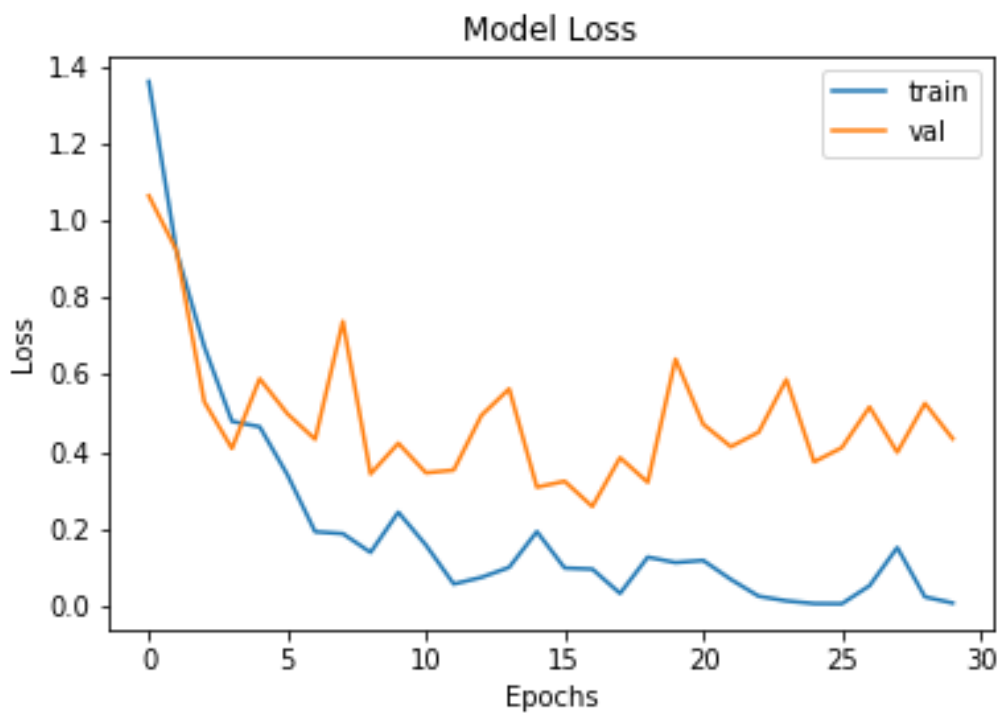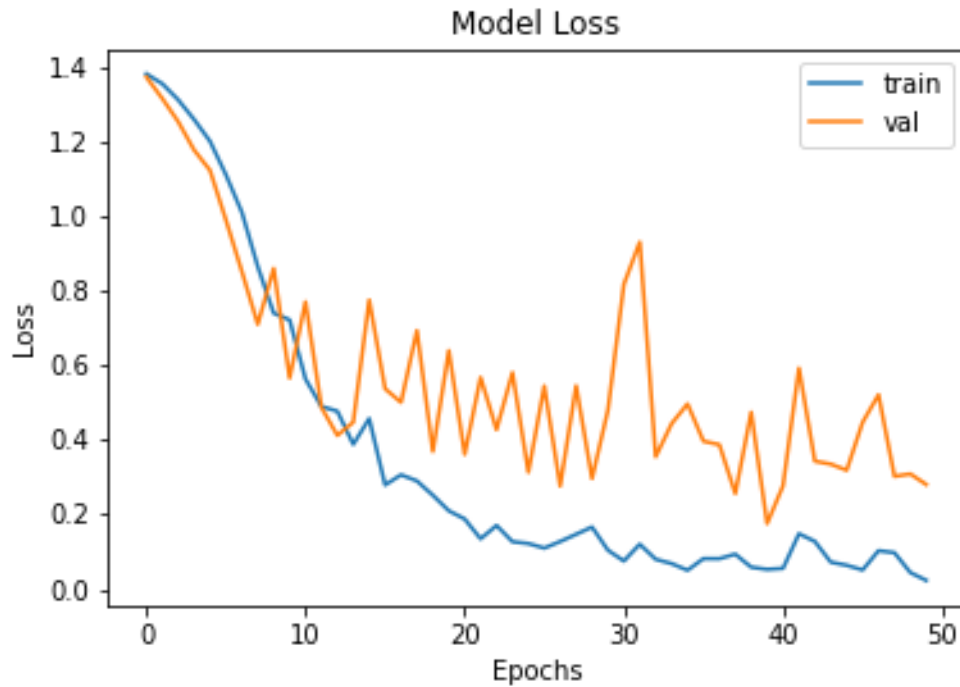**Figure 4. 15** Loss curve across the training and validation process for ResNet50 Model
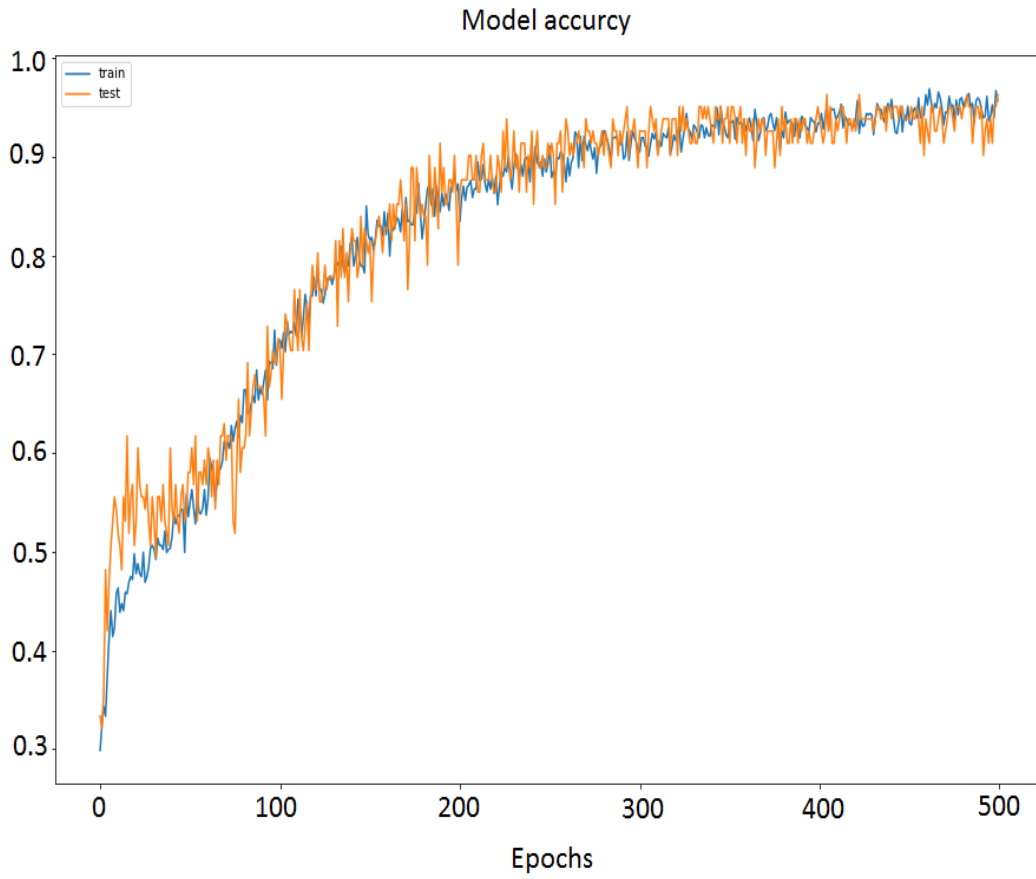
Figure 4. 16 Accuracy curve across the training and validation process for Proposed CNN Model
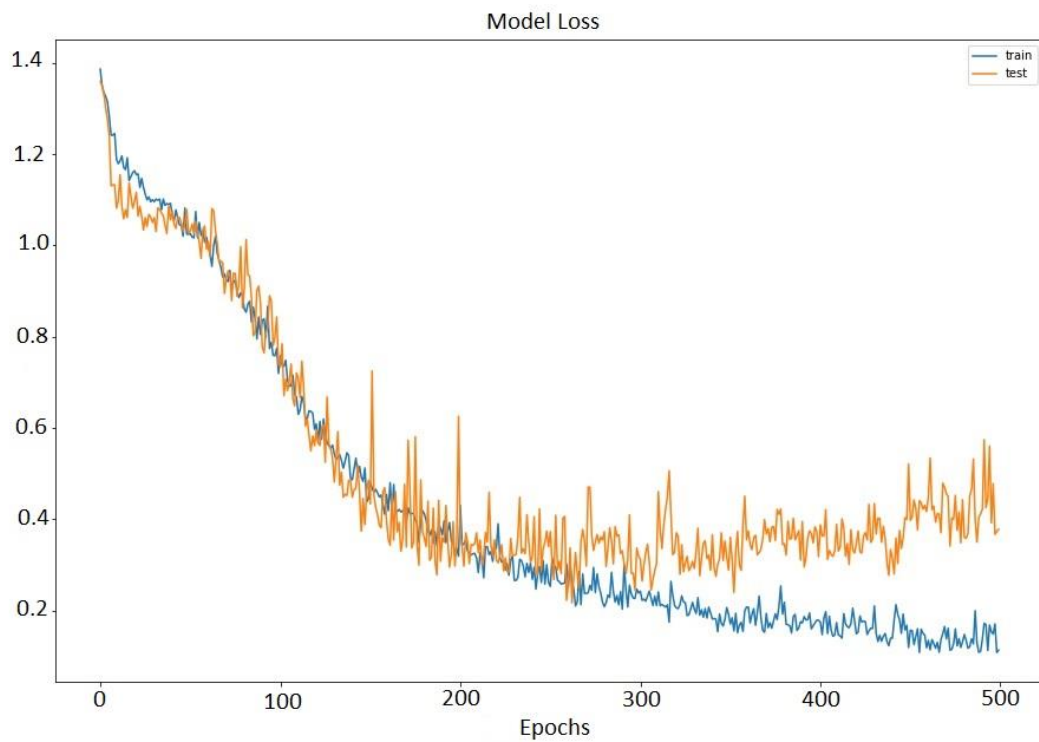
4.1 DISCUSSION

This study offered an automatic identification approach for recognizing and categorizing urine sediment images based on machine learning and deep learning methodologies. The categorization was applied to four types of cells in urine sediment. In certain circumstances, creating a genuine data set is more laborious and difficult to obtain data, but it can have claimed that it is more worthy of your aims, and your methods may be utilized for actual data in the future, Because of those reasons for this study real dataset was used.

Gathering microscope urine images and prepared real dataset was a first step of this study. Manually collect images in a public Shorsh Hospital in Sulaymanyah city and Shifa Private Laboratory in Ranya city. Duration of collect data it took more than three months. When collecting the data appeared some limitations which are explained it on the Chapter Five. Totally from these two labs 1,420 urine sediment images are gathered. Because of noise on images removing several images remained 820 images, cut the images and focused on four cell types; containing RBC, Calcium Oxalate, Cysten Crystal and Uric acid Crystal. Image processing is more significant in a medical image. So for simplifying and clearer conversion of RGB images to gray scale and threshold operation are done. Following successful image preprocessing, the datasets were separated into training and testing sets. The training set got 80% of the dataset, whereas the testing set got 20%.

Eight different models were trained on the prepared real dataset. Two methods to train on the dataset are performed. First, the image dataset directly goes to classifying algorithms for that method proposed CNN model and five type of CNN Transfer learning model. The compering of these models, they have good performance and good results but CNN transfer learning speedily than Proposed CNN model needs a few epochs to get a good result.

In the second method the image dataset does not directly go to classifying algorithms, feature extraction was performed, extracts 22 features and prepared numeric dataset. After normalizing the numeric dataset go to scanning algorithms, for that method perform SVM and KNN algorithms.

The performance of any developed algorithm is critical. As a result, the performance of the models was tested and compared using measures such as accuracy, recall, precision, and F1 score. The confusion matrix was also computed for each model. The results show the best model is CNN transfer learning MobileNet model. This model achieved the highest accuracy of 98.3%. Also, InceptionV3 and DenceNet have comparable accuracy results with 97.5%. And the proposed CNN structure has a good result with 96.12%. For comparing these two methods that used in this study, the first method is slow but it has shown better result than the second method and does not need to perform feature extraction. Because the dimensionality reduction technique is ideally matched to the vast number of parameters in an image, CNN is particularly successful for image classification. The second technique is faster, but the performance is not superior, and it requires feature extraction from images.

When compared to traditional artificial microscopy identification techniques and other automatic authentication techniques, the findings of this study show high accuracy, achieving automation and standardization of urine sediment detection, greatly speeding up urine sample detection and improving work efficiency, reducing human error, and ensuring the quality of urine samples tested. This study also compared to earlier studies that achieved the greatest results by utilizing a limited dataset. Previous studies needed thousands of samples and a large dataset to achieve a decent outcome.

CHAPTER FIVE

CONCLUSION AND FUTURE WORK

5.1 CONCLUSION

This chapter presents the summary of this thesis; also, it proposes some directions for further work that could achieve further ways to improve the efficiency of the proposed system.

This study presented a thorough method for automating techniques for identifying and classifying microscopic urine components. This method integrated 820 cell annotations from four cell types observed in microscopic images of urine sediment: RBC, Calcium oxalate, Cysten Calcium, and Uric acid. Two approaches for evaluating urine sediment images were tested. Many important conclusions have been obtained from implementing and applied the proposed urine analyzing technique including:

1. The proposed method, which has been used in this thesis for classification, is a universal method because it can be applied generally. Which means it can apply to any other fields, just by adding the related dataset to the desired goal.

2. In general, clinicians and patients would benefit greatly from an automated method that can analyze and classify urine sample images. The automated method it benefits in time, reduce labor insensitive and more accurate also no need cost.

3. The two approaches that have been implemented in this study, there are quick with an acceptable time with high performance.

4. Taken a good number of original urine sediment images with high resolution, prepared a good real dataset. It can be applies and tests to any other methods, just by adding the dataset to the algorithms.

5.2 LIMITATIONS OF THIS STUDY ARE:

1. The inability to capture all predicted urine particles, some of which are not being visible in any imaging and others are too tiny to study.

2. Images will be taken manually, with no automation.

3. It will not cover the detection of moving things such as germs.

4. This research will not solve overlapping and contacting particles that cannot be separated using a standard segmentation approach.

5.3 FUTURE RECOMMENDATIONS

This study was one of the strategies for detecting and classifying urine sediment images that achieved pretty satisfactory and much greater accuracy than clinical testing. It was also more accurate than any other contemporary tests that could be classed. Here are a few suggestions for future work that may be investigated at further:

1. Many particles will be gathered and investigated among those that were not evaluated by this research; this will necessitate further efforts and the employment of several cameras in other medical labs. Furthermore, because manual labeling was a time-consuming process in this investigation, a team of professionals was assembled to manually identify images.

2. After segmentation and thresholding, overlapping and contacting particles yield indeterminate shapes of particles. This issue raised the mistake rate, and developing a way to divide contacting particles or remove some particle from overlapping will improve classification results.

3. The study would like to recommend the use of the same convolution network models for classification and identification difficulties using microscopic video of urine sediment

References

AL-SAFFAR, A. A. M., TAO, H. & TALAB, M. A. Review of deep convolution neural network in image classification. 2017 International conference on radar, antenna, microwave, electronics, and telecommunications (ICRAMET), 2017. IEEE, 26-31.

ALBAWI, S., MOHAMMED, T. A. & AL-ZAWI, S. Understanding of a convolutional neural network. 2017 international conference on engineering and technology (ICET), 2017. Ieee, 1-6.

ALMADHOUN, M. D. & EL-HALEES, A. 2014. Automated recognition of urinary microscopic solid particles. *Journal of medical engineering & technology,* 38**,** 104-110.

AO, S.-I., RIEGER, B. B. & AMOUZEGAR, M. 2010. *Machine learning and systems engineering*, Springer Science & Business Media.

APOLLONI, B., GHOSH, A., ALPASLAN, F. & PATNAIK, S. 2005. *Machine learning and robot perception*, Springer Science & Business Media.

BALBIN, J. J. R., MAGWILI, G. V., VALIENTE JR, L. D., GAWARAN, D. L. B., LUMAPAS, N. E. R. & UMALI, A. M. Detection and Identification of Triple Phosphate Crystals and Calcium Oxalate Crystals in Human Urine Sediment Using Harr Feature, Adaptive Boosting and Support Vector Machine via Open CV. Proceedings of the 2020 10th International Conference on Biomedical Engineering and Technology, 2020. 34-39.

BALL, R., GERAKOS, J., LINNAINMAA, J. T & .NIKOLAEV, V. 2020. Earnings, retained earnings, and book-to-market in the cross section of expected returns. *Journal of Financial Economics,* 135**,** 231-254.

BASHA, S. S., DUBEY, S. R., PULABAIGARI, V. & MUKHERJEE, S. 2020. Impact of fully connected layers on performance of convolutional neural networks for image classification. *Neurocomputing,* 378**,** 112-119.

BISHOP, C. M. & NASRABADI, N. M. 2006. *Pattern recognition and machine learning*, Springer.

CAO, G., ZHONG, C., LI, L. & DONG, J. Detection of red blood cell in urine micrograph. 2009 3rd International Conference on Bioinformatics and Biomedical Engineering, 2009. IEEE, 1-4.

CIREGAN, D., MEIER, U. & SCHMIDHUBER, J. Multi-column deep neural networks for image classification. 2012 IEEE conference on computer vision and pattern recognition, 2012. IEEE, 3642-3649.

CLEOPHAS, T. J., ZWINDERMAN, A. H. & CLEOPHAS-ALLERS, H. I. 2013. *Machine learning in medicine*, Springer.

CRUZ, J. C. D., GARCIA, R. G., AVILLEDO, M. I. D., BUERA, J. C. M., CHAN, R. V. S. & ESPANA, P. G. T. Microscopic Image Analysis and Counting of Red Blood Cells and White Blood Cells in a Urine Sample. Proceedings of the 2019 9th International Conference on Biomedical Engineering and Technology, 2019. 113-118.

DAHL, G. E., YU, D., DENG, L & .ACERO, A. 2011. Context-dependent pre-trained deep neural networks for large-vocabulary speech recognition. *IEEE Transactions on audio, speech, and language processing,* 20**,** 30-42.

DANJUMA, K. J. 2015. Performance evaluation of machine learning algorithms in post-operative life expectancy in the lung cancer patients. *arXiv preprint arXiv:1504.04646*.

DE BOER, F. J., GIETELING, E., VAN EGMOND-KREILEMAN, H., MOSHAVER, B., VAN DER LEUR, S. J., STEGEMAN, C. A. & GROENEVELD, P. H. 2017. Accurate and fast urinalysis in febrile patients by flow cytometry. *Infectious Diseases,* 49**,** 380-387.

DONG, S., ZHANG, S., JIAO, L. & WANG, Q. Automatic Urinary Sediments Visible Component Detection Based on Improved YOLO Algorithm. 2020 International Conference on Computer Vision, Image and Deep Learning (CVIDL), 2020. IEEE, 485-490.

EL NAQA, I. & MURPHY, M. J. 2022. What Are Machine and Deep Learning? *Machine and Deep Learning in Oncology, Medical Physics and Radiology.* Springer.

ESTEVA, A., KUPREL, B., NOVOA, R. A., KO, J ,.SWETTER, S. M., BLAU, H. M. & THRUN, S. 2017. Dermatologist-level classification of skin cancer with deep neural networks. *nature,* 542**,** 115-118.

GINARDI, R., SAIKHU, A., SARNO, R., SUNARYONO, D., KHOLIMI, A. S. & SHANTY, R. N. T. Intelligent method for dipstick urinalysis using smartphone camera. Information and Communication Technology-EurAsia Conference, 2014. Springer, 66-77.

GONG, Y. & XU, W. 2007. *Machine learning for multimedia content analysis*, Springer Science & Business Media.

GOSWAMI, D., AGGRAWAL, H. & AGARWAL, V. Cell Detection and Classification from Urine Sediment Microscopic Images.

GUO, G., WANG, H., BELL, D., BI, Y. & GREER, K. KNN model-based approach in classification. OTM Confederated International Conferences" On the Move to Meaningful Internet Systems", 2003. Springer, 986-996.

HE, K., ZHANG, X., REN, S. & SUN, J. Deep residual learning for image recognition. Proceedings of the IEEE conference on computer vision and pattern recognition, 2016. 770-778.

HUANG, G., LIU, Z., VAN DER MAATEN, L. & WEINBERGER, K. Q. Densely connected convolutional networks. Proceedings of the IEEE conference on computer vision and pattern recognition, 2017. 4700-4708.

HUANG, S., CAI, N., PACHECO, P. P., NARRANDES, S., WANG, Y. & XU, W. 2018. Applications of support vector machine (SVM) learning in cancer genomics. *Cancer genomics & proteomics,* 15**,** 41-51.

İNCE, F. D., ELLIDAĞ, H. Y., KOSEOĞLU, M., ŞIMŞEK, N., YALÇıN, H. & ZENGIN, M. O. 2016. The comparison of automated urine analyzers with manual microscopic examination for urinalysis automated urine analyzers and manual urinalysis. *Practical laboratory medicine,* 5**,** 14-20.

JI, Q., LI, X., QU, Z. & DAI, C. 2019. Research on urine sediment images recognition based on deep learning. *IEEE Access,* 7**,** 166711.166720-

JIANG, X., CHEN, F., CHEN, Q., SI, M. & WANG, W. Texture segmentation of urinary sediment image based on a weighted Gaussian mixture model with Markov random fields. Proceedings of the 2018 7th International Conference on Bioinformatics and Biomedical Science, 2018. 82-87.

KABIR, M. 2019. Predictive analysis on Standard Health Deficiency with Support Vector Machine using Confusion Matrix.

KANG, R., LIANG, Y., LIAN, C. & MAO, Y. 2018. CNN-based automatic urinary particles recognition. *arXiv preprint arXiv:1803.02699.*

KEKRE, H., SARODE, T. K. & GHARGE, S. M. 2009. Tumor detection in mammography images using vector quantization technique. *International Journal of Intelligent Information Technology Application,* 2**,** 237-242.

KERMANY, D. S., GOLDBAUM ,M., CAI, W., VALENTIM, C. C., LIANG, H., BAXTER, S. L., MCKEOWN, A., YANG, G., WU, X. & YAN, F. 2018. Identifying medical diagnoses and treatable diseases by image-based deep learning. *Cell,* 172**,** 1122-1131. e9.

KIM, P. 2017. Convolutional neural network .*MATLAB deep learning.* Springer.

KRISHNA, S. T. & KALLURI, H. K. 2019. Deep learning and transfer learning approaches for image classification. *International Journal of Recent Technology and Engineering (IJRTE),* 7**,** 427-432.

KRIZHEVSKY, A., SUTSKEVER, I & .HINTON, G. E. Imagenet classification with deep convolutional neural networks. Advances in neural information processing systems, 2012. 1097-1105.

LAIWEJPITHAYA, S., WONGKRAJANG, P., REESUKUMAL, K., BUCHA, C., MEEPANYA, S., PATTANAVIN, C., KHEJONNIT, V & .CHUNTARUT, A. 2018. UriSed 3 and UX-2000 automated urine sediment analyzers vs manual microscopic method: A comparative performance analysis. *Journal of clinical laboratory analysis,* 32**,** e22249.

LAKATOS, J., BODOR, T., ZIDARICS, Z. & NAGY, J. 2000. Data processing of digital recordings of microscopic examination of urinary sediment. *Clinica chimica acta,* 297**,** 225-237.

LAMCHIAGDHASE, P., PREECHABORISUTKUL, K., LOMSOMBOON, P., SRISUCHART, P., TANTINITI, P. & PREECHABORISUTKUL, B. 2005. Urine sediment examination: a comparison between the manual method and the iQ200 automated urine microscopy analyzer. *Clinica Chimica Acta,* 358**,** 167-174.

LECUN, Y., BOTTOU, L., BENGIO, Y. & HAFFNER, P. 1998. Gradient-based learning applied to document recognition. *Proceedings of the IEEE,* 86**,** 2278-2324.

LI, H.-R., HE, F.-Z. & YAN, X.-H. 2019a. IBEA-SVM: an indicator-based evolutionary algorithm based on pre-selection with classification guided by SVM. *Applied Mathematics-A Journal of Chinese Universities,* 34**,** 1-26.

LI, K ,.LI, M., WU, Y., LI, X. & ZHOU, X. An Accurate Urine Erythrocytes Detection Model Coupled Faster RCNN with VggNet. Proceedings of the 2020 Conference on Artificial Intelligence and Healthcare, 2020a. 224-228.

LI, Q., YU, Z., QI, S., HE, Z., LI, S. & GUAN ,H. A recognition method of urine cast based on deep learning. 2019 International Conference on Systems, Signals and Image Processing (IWSSIP), 2019b. IEEE, 157-161.

LI, Q., YU, Z., QI, T., ZHENG, L., QI, S., HE, Z., LI, S. & GUAN, H. 2020b. Inspection of visible components in urine based on deep learning. *Medical Physics,* 47**,** 2937-2949.

LI, T., JIN, D., DU, C., CAO, X., CHEN, H., YAN, J., CHEN, N., CHEN, Z., FENG, Z. & LIU, S. 2020c. The image-based analysis and classification of urine sediments using a LeNet-5 neural network. *Computer Methods in Biomechanics and Biomedical Engineering: Imaging & Visualization,* 8**,** 109-114.

LIANG, Y., KANG, R., LIAN, C. & MAO, Y. 2018a. An end-to-end system for automatic urinary particle recognition with convolutional neural network. *Journal of medical systems,* 42**,** 1-14.

LIANG, Y., TANG, Z., YAN, M. & LIU, J. 2018b. Object detection based on deep learning for urine sediment examination. *Biocybernetics and Biomedical Engineering,* 38**,** 661-670.

LIU, W., LI, W. & GONG, W. 20 .20Ensemble of fine-tuned convolutional neural networks for urine sediment microscopic image classification. *IET Comput. Vis.,* 14**,** 18-25.

MADHAVAN, S. & JONES, M. T. 2017. Deep learning architectures. *línea]. Available: https://developer. ibm. com/technologies/deep-learning/articles/.[Último acceso: 02 Junio 2021.*

MAHESH, B. 2020. Machine learning algorithms-a review. *International Journal of Science and Research (IJSR).[Internet],* 9**,** 381-386.

MAHMOUD, T. A. & MARSHALL, S. Medical image enhancement using threshold decomposition driven adaptive morphological filter. 2008 16th European Signal Processing Conference, 2008. IEEE, 1-5.

MALLEY, J. D., MALLEY, K. G. & PAJEVIC, S. 2011. *Statistical learning for biomedical data*, Cambridge University Press.

MERAJ ,S. S., YAAKOB, R., AZMAN, A., RUM, S., SHAHREL, A., NAZRI, A. & ZAKARIA, N. F. 2019. Detection of pulmonary tuberculosis manifestation in chest X-rays using different convolutional neural network (CNN) models. *Int. J. Eng. Adv. Technol.(IJEAT),* 9**,** 2270.2275-

MITRA, S., DATTA, S., PERKINS, T. & MICHAILIDIS, G. 2008. *Introduction to machine learning and bioinformatics*, CRC Press.

MOHAMAD, M. A., HASSAN, H., NASIEN, D. & HARON, H. 2015. A review on feature extraction and feature selection for handwritten character recognition. *International Journal of Advanced Computer Science and Applications,* 6.

NAIR, M. & BINDHU, J. 2016. Supervised techniques and approaches for satellite image classification. *International Journal of Computer Applications,* 134.

OYAERT ,M. & DELANGHE, J. 2019. Progress in automated urinalysis. *Annals of laboratory medicine,* 39**,** 15-22.

PAN, J., JIANG, C. & ZHU, T. Classification of urine sediment based on convolution neural network. AIP Conference Proceedings, 2018. AIP Publishing LLC.040176 ,

QU, Z., CAI, S., JI, Q. & XU, L. Lightweight Urine Sediment Image Recognition Network Based on Deep Separable Residual Structure. 2021 IEEE 15th International Conference on Electronic Measurement & Instruments (ICEMI), 2021. IEEE, 152-157.

RAFIQ ,R. B. & ALBERT, M. V. 2022. Transfer Learning: Leveraging Trained Models on Novel Tasks. *Bridging Human Intelligence and Artificial Intelligence.* Springer.

RAHMAT, R., MUCHTAR, M., TAQIUDDIN, R., ADNAN, S., ANUGRAHWATY, R. & BUDIARTO, R. Automated color classification of urine dipstick image in urine examination. Journal of Physics: Conference Series, 2018. IOP Publishing, 012008.

SAJEDI, H., MOHAMMADIPANAH, F. & PASHAEI, A. 2020. Image-processing based taxonomy analysis of bacterial macromorphology using machine-learning models. *Multimedia Tools and Applications,* 79**,** 32711-32730.

SANGHVI, A. B., ALLEN, E. Z., CALLENBERG, K. M. & PANTANOWITZ, L. 2019. Performance of an artificial intelligence algorithm for reporting urine cytopathology. *Cancer cytopathology,* 127**,** 658-666.

SARAVANAN, R. & SUJATHA, P. A state of art techniques on machine learning algorithms: a perspective of supervised learning approaches in data classification. 2018 Second International Conference on Intelligent Computing and Control Systems (ICICCS), 2018. IEEE, 945-949.

SHEN, D., WU, G. & SUK, H.-I. 2017. Deep learning in medical image analysis. *Annual review of biomedical engineering,* 19**,** 221.

SHETTY, S. & RAO, Y. SVM based machine learning approach to identify Parkinson's disease using gait analysis. 2016 International Conference on Inventive Computation Technologies (ICICT), 2016. IEEE, 1-5.

SHMILOVICI, A. 2009. Support vector machines. *Data mining and knowledge discovery handbook.* Springer.

SIMONYAN, K. & ZISSERMAN, A. 2014. Very deep convolutional networks for large-scale image recognition. *arXiv preprint arXiv:1409.1556.*

SONG, Z., FU, L., WU, J., LIU, Z., LI, R. & CUI, Y. 2019. Kiwifruit detection in field images using Faster R-CNN with VGG16. *IFAC-PapersOnLine,* 52**,** 76-81.

SUN ,Q., YANG, S., SUN, C. & YANG, W. An automatic method for red blood cells detection in urine sediment micrograph. 2018 33rd Youth Academic Annual Conference of Chinese Association of Automation (YAC), 2018. IEEE, 241-245.

TENG, L., LI, H. & KARIM, S. 201 .9DMCNN: A deep multiscale convolutional neural network model for medical image segmentation. *Journal of Healthcare Engineering,* 2019.

TORREY, L. & SHAVLIK, J. 2010. Transfer learning. *Handbook of research on machine learning applications and trends: algorithms, methods, and techniques.* IGI global.

VELASCO, J. S., CABATUAN, M. K. & DADIOS, E. P. 2019. Urine sediment classification using deep learning. *Lecture Notes on Advanced Research in Electrical and Electronic Engineering Technology***,** 180-185.

WAHID ,M. F., HASAN, M. J., ALOM, M. S. & MAHBUB, S. Performance Analysis of Machine Learning Techniques for Microscopic Bacteria Image Classification. 2019 10th International

Conference on Computing, Communication and Networking Technologies (ICCCNT), 2019. IEEE, 1-4.

WÄLDCHEN, J. & MÄDER, P. 2018. Machine learning for image based species identification. *Methods in Ecology and Evolution,* 9**,** 2216-2225.

WANG, Q., SUN, Q. & WANG, Y. A two-stage urine sediment detection method. 2020 International Conference on Image, Video Processing and Artificial Intelligence, 2020. International Society for Optics and Photonics, 1158404.

WANG, S., JIANG, Y., HOU, X., CHENG, H. & DU, S. 2017. Cerebral micro-bleed detection based on the convolution neural network with rank based average pooling. *IEEE Access,* 5**,** 16576-16583.

WANG, W., CHEN, F., LIU, X., LIU, H., HU, T. & YANG, L. Study on segmentation and recognition algorithm of crystal in urinary sediment image. Eleventh International Conference on Digital Image Processing (ICDIP 2019), 2019. International Society for Optics and Photonics, 111791J.

WESARACHKITTI, B., KHEJONNIT, V., PRATUMVINIT, B., REESUKUMAL, K., MEEPANYA, S., PATTANAVIN, C. & WONGKRAJANG, P. 2016. Performance evaluation and comparison of the fully automated urinalysis analyzers UX-2000 and Cobas 6500. *Laboratory Medicine,* 47**,** 124-133.

WU, P., ZHU, M., PU, P. & JIANG, T. An Adaptive Sampling Ensemble Learning Method for Urinalysis Model. 2010 2nd International Conference on Information Engineering and Computer Science, 2010. IEEE, 1-4.

WU, Z. & JI, Q. Urine sediment image recognition method based on re-parameterization network. International Conference on Signal Processing and Communication Technology (SPCT 2021), 2022. SPIE, 64-70.

WUEST, T., WEIMER, D., IRGENS, C. & THOBEN, K.-D. 2016. Machine learning in manufacturing: advantages, challenges, and applications. *Production & Manufacturing Research,* 4**,** 23-45.

XIANG, H., CHEN, Q., WU, Y., XU, D., QI, S., MEI, J., LI, Q. & LIU, X. Urine Calcium oxalate crystallization recognition method based on deep learning. 2019 International Conference on Automation, Computational and Technology Management (ICACTM), 2019. IEEE, 30-33.

YANG, Z. R. 2010. *Machine learning approaches to bioinformatics*, World scientific.

YU ,J. & TAO, D. 2013. *Modern machine learning techniques and their applications in cartoon animation research*, John Wiley & Sons.

ZHANG, S., LI, X., ZONG, M., ZHU, X. & CHENG, D. 2017. Learning k for knn classification. *ACM Transactions on Intelligent Systems and Technology (TIST),* 8**,** 1-19.

ZHANG, X., JIANG, L., YANG, D., YAN, J. & LU, X. 2019. Urine sediment recognition method based on multi-view deep residual learning in microscopic image. *Journal of Medical Systems,* 43**,** 1-10.

ZHENG, L., LI, G. & BAO, Y. Improvement of grayscale image 2D maximum entropy threshold segmentation method. 2010 International Conference on Logistics Systems and Intelligent Management (ICLSIM), 2010. IEEE, 324-328.

ZHENG, Q., FURTH, S. L., TASIAN, G. E. & FAN, Y. 2019. Computer-aided diagnosis of congenital abnormalities of the kidney and urinary tract in children based on ultrasound imaging data by integrating texture image features and deep transfer learning image features. *Journal of pediatric urology,* 15**,** 75. e1-75. e7.

ZHUANG, F., QI, Z., DUAN, K., XI, D., ZHU, Y., ZHU, H., XIONG, H. & HE, Q. 2020. A comprehensive survey on transfer learning. *Proceedings of the IEEE,* 109**,** 43-76.

Urine Sediment Analysis by Using Convolution Neural Network

Zhwan Mohammed Khalid
Department of Information System Engineering Techniques
Erbil Technical Engineering College
Erbil Polytechnic University
Erbil, Iraq
Zhwan.mohammed@uor.edu.krd

Roojwan Scddeek Hawezi
Department of Information System Engineering Techniques
Erbil Technical Engineering College
Erbil Polytechnic University
Erbil, Iraq
roojwan.hawezi@epu.edu.iq

Sara Raouf Muhamad Amin
Department of Information System Engineering Techniques
Erbil Technical Engineering College
Erbil Polytechnic University
Erbil, Iraq
sara.muhamad@epu.edu.iq

Abstract— Urinary particles are important requirements in clinical urinalysis, particularly in the diagnosis and monitoring of patients suspected of renal diseases and urinary tract Infections. As a result, it is critical to identify urinary particles accurately in the clinical area. Also the outcome is hugely affected by the doctor's experience. However, because the traditional manual microscopic analysis relies on human operators who read the samples visually and identify them, this method is slow, time-consuming, and labor-intensive. In this research, presented a deep learning method for analyzing urinary particles. The authors prepare a dataset of urine sediment microscopic images, which includes approximately 820 cell annotations and four-cell classes: RBC, Calcium oxalate, cysteine calcium, and uric acid. Used for deep learning training and testing of various convolutional network models. The authors proposed Convolution neural network structure and five ConvNet models such as MobileNet, VGG16, DenseNet, ResNet50V, InceptionV3. According to these evaluations, the best models for true positive recall are MobileNet, and the proposed method ist he second one.. These models also achieve the highest accuracy of 98.3 percent. on the other hand, InceptionV3 and DenceNet have comparable accuracy results with 96.5 percent.

Keywords— *CNN, Microscopic Image,, Transfer Learning, Urine Analysis, Urine Sediment.*

I. INTRODUCTION

Urinalysis is essential for the accurate identification of renal and urinary tract disorders. Its goal is to gather information on the number of particles in urine sediment, which is mostly consisting of calcium (Oxalate, cysteine, uric acid, Phosphate), mucus, Blood Cells such as red blood cells and white blood cells, and Casts[1, 2]. Urine sample analysis is critical in clinical screening, diagnosis, and public health promotion. Because a patient's urine sample differs from that of a healthy individual, the analysis can successfully aid in the identification of urinary problems. In general, the RBC count may be used to detect disorders associated with haematuria, Inflammation of the kidneys and bladder, renal tuberculosis, and other conditions. Red blood cell (RBC) morphology can be used to indicate the location and kind of kidney illness[3]. Traditional urine microscopic inspection requires the employment of qualified laboratory professionals.

Furthermore, Urine analysis is time-consuming and labor-intensive, and it is easily impacted by laboratory physicians' subjective will and working weariness[4]. With the advancement of digital picture technology, an experienced person holds can only process 100 samples per day, which is insufficient to fulfill today's clinic requirements. Automated image recognition has become increasingly popular in the field of medicine[5, 6]. The traditional approach, based on "target segmentation feature selection and extraction classifier," has made some success in identifying and detecting urine sediment pictures[7]. The usefulness of these strategies is mostly determined by the accuracy of target segmentation and the efficiency of feature selection and aggregation. Urine sediment photographs include less distinguishing elements apparent to the human eye when compared to other common images, and certain categories have a high degree of similarity. As a result, breaking past the bottleneck of high-accuracy classification using standard approaches is difficult. The authors presented a convolutional neural network (CNN)-based approach for automated analysis of urine sample pictures in this study. CNN's can identify patterns in pictures without the need for further pre-processing. When it comes to spotting patterns that have experienced basic geometric deformation, CNNs are highly durable. CNN's provide several advantages over normal neural networks in image processing, including a strong match between the image input and the network's topological structures, as well as integrated feature extraction and sequence classification. Furthermore, weight sharing allows for fewer parameters in training, resulting in a very simple network component with good adaptability. The rest of this paper is arranged as follows: The first section introduction about urinalysis. Section II discuss of previous work related to urinalysis. In the section III the methods and materials are discussed. Study results are described in section IV. Lastly, conclusion is presented.

II. RELATED WORK

In 2019, Xiang et al. [8] based on the entire convolution neural network, proposed a new identification approach for microscopic examination of CaOx crystals in urine samples. This method can detect the image of a microscopic

بەراوردکردنی چەند ئەلگۆریثمێکی جیاوازی دییپ لێرنینگ بۆ سیستەمی ناسینەوەی شیکردنەوەی میز

نامەیەکە

پێشکەشی ئەنجومەنی کۆلێژی تەکنیکی ئەندازیاری هەولێر کراوە لە زانکۆی پۆلیتەکنیکی هەولێر وەکو بەشێك لە پێداویستیەکانی بەدەستهێنانی ماستەر لە ئەندازیاری سیستەمی زانیاریەکان

لەلایەن

ژوان محمد خالد

بەکالۆریۆس لە ئەندازیاری پرۆگرامسازی

به سەرپەرشتیاری

د. روجوان صدیق ئیسماعیل

د. سارە رؤوف محمدامین

پوخته

پشکنینی میکرۆسکۆپی میز زۆر گرنگه بۆ دهستنیشانکردن و چاودێریکردنی ئەو کەسانەی گومانیان لێکراوه که نەخۆشیی گورچیله یان هەوکردنی میزیان هەیه. به شێوهیەکی گشتی، دڵۆپێک میز له ژێر مایکرۆسکۆپێکدا تاقی دهکرێنەوه بۆ ژماردن و پۆلێنکردنی پێکهاتەکانی ناو میز. ئەمه پرۆسەیەکی کاتی دهوێت ودهبێتە هۆی دروست بوونی قەڵەبالغی له تاقیگەکان وه پێویستی به کەسی شارهزاو دابینکردنی بودجەیەکه بۆ ئەو کەسەی که پێکهاتەکان دهخوێنێتەوه لەسەر مایکرۆسکۆپەکه کار دهکات. پزیشکیەکان و نەخۆشەکان سوودێکی زۆر وەردهگرن له شێوازی ئۆتۆماتیکی که دهتوانێت وێنەی نموونەی میز شی بکاتەوه و چەندایەتی بکات.

لەم توێژینەوهیەدا ئەلگۆریثمەکانی دیب لێرنینگ بەکارهاتووه بۆ شیکردنەوهی میز. له هەنگاوی یەکەمدا به کۆکردنەوهی وێنەکانی پێکهاتەکانی میز له ژێر مایکرۆسکۆپ داتاسێتێك ئامادهکراوه که پێکهاتووه له ٨٢٠ وێنەی بۆ چوار پۆلی خانه: RBC، کالسیۆم ئۆکسالات، سیستین کالسیۆم، و ترشی یوریک.له هەنگاوی دواتردا هەندێک کار لەسەر وێنەکان کراوه بۆ ئەوهی روونتر بن چاکتر بناسرین و ئەنجامێکی باش بەدهست بێت. بۆ ئەم توێژینەوهیه دوو رێگا بۆ شیکردنەوهی وێنەکانی ئەم چوار پێکهاتەی میز پێشکەش کراوه. یەکەم، پرۆپۆسی CNN مۆدێل و پێنج مۆدێلی کۆنڤۆ نێت وەک MobailNet، VGG16، DenseNet، ResNet50V و InceptionV3، بەکارهاتووه لەم میتودیدا دوای ئەوهی هەندێ کار لەسەر وێنەکان کراوه بۆ روون بوونیان راستەوخۆ ئەمجێت بۆ پشکنینی ئەلگۆریثمەکان. لەمیتۆدی دووهمدا پێش ئەوهی وێنەکان بچنه ناو ئەلگۆریثمەکان بۆ پشکنینیان دهرهێنانی خاسیەتی وێنەی لەسەر ئەنجام دراوه. که 22 تایبەتمەندی گرینگەکانی وێنەی لێ دهرهێنراوه له ، بەمەش داتاسێتێکی ژمارهیی ئامادهکراوه که شیتێکی ئیگزل فایله ، پێکهاتووه له ٨٢٠ ریزی ئاسۆیی که هەر یەک له ریزهکان تایبەتمەندی وێنەیەک نیشان دهدات وه ٢٣ ریزی ستونی که ٢٢ دانه تایبەتمەندی وێنەکانه وه ستونی کۆتایی بریتیه له لەیبڵ بۆ هەر وێنەیەک. پاشان داتاسێتەکه پرۆسەی نۆرمەڵایزی لەسەر جێبەجێ کراوه. له کۆتایدا، داتاسێتەکه به ئەلگۆریثم ناساندراوه بۆ جیاکردنەوهی بابەتەکان. بۆ ئەو مەبەستە دوو ئەلگۆریثمی جیاواز بەکارهاتووه که بریتین له (SVM) و (KNN).

باشترین مۆدێل مۆبایل نێته. ئەم مۆدێلانه بەرزترین رێژهی له سەدا ٩٨,٣ بەدهست دههێنن هەروەها InceptionV3 و DenseNet ئەنجامێکی وردی بەراوردکراویان هەیه که 97.5٪ هەروەها پێکهاتەی پێشنیارکراوی سی ئێن ئێن ئەنجامێکی باشی هەیه به ٩٦,١٢٪ ئەم توێژینەوهیه سوودێکی زۆری دهبێت بۆ پزیشکیەکان بۆ شیکردنەوهی ئۆتۆماتیکی و دهستنیشان کردنی وێنەکانی پێکهاتەی میز.